Dear Referee,

We thank the referee for taking the time to provide such a constructive and thorough review of our manuscript (GMD-2023-173). According to the suggestive comments, we have made some modifications to the manuscript, and the responses are listed below. To guide the review process, comments from the referee and original texts in the manuscript are presented in black, our responses are in blue, and any text modifications made to the manuscript are highlighted in red italics. Links are provided below for easy navigation in the document.

We are looking forward to your reply.

Best regards,
Yours sincerely
Sheng Fang

General comments

The paper presented a source reconstructing procedure by first locating the source location before estimating the emission rates. A machine learning method has been used in the first step to locate the source location. The overall results are quite interesting and encouraging.

However, there are several shortcomings in this manuscript. Some of the statements are not accurate and some terminology uses are also questionable. The presentation of the machine learning method is not easy to follow for those who are not quite familiar with the same method and software. In addition, the dispersion model errors affect the results but are not sufficiently considered or discussed. It is also a concern that the method is only tested with a single set of experimental data. More test cases are probably needed.

Response to general comments:

Thank you for your valuable feedback and suggestive comments on our manuscript. We are particularly grateful for your remarks about our results being "quite interesting and encouraging". We have addressed the issues you have raised and revised the manuscript accordingly, which are detailed as follows:

(1) Inaccurate statements and terminology use:

Following your comments, we have thoroughly reviewed our manuscript and corrected all statements that were inaccurate or unclear. Particularly, we have elaborated and rephrased the "Spatiotemporally-decoupled" and "constant-release assumption" in the introduction section as "*Spatiotemporally-separated*" and "*Assumptions on the release characteristics*", respectively. Moreover, the title of the revised manuscript has been changed to "*A spatiotemporally-separated framework for reconstructing the source of atmospheric radionuclide releases*" to better describe the current two-step method. More detailed revisions are provided in the response to your specific comments. Regarding the use of terminology, we have provided clear definitions and detailed explanations, such as:

(1.1) Line 15 of section "Abstract": "source localization"

The term "source localization" has been replaced with "source location estimation" in the revised manuscript. For example,

► Line 15 of section "Abstract" has been replaced with:

"A machine learning model is trained to link these features to the source location, enabling independent *source location estimation*."

► Line 94-97 of section "1. Introduction" has been replaced with:

"The performance of the proposed method is compared with the correlation-based method for *source location estimation* and the Bayesian method for spatiotemporal accuracy. The sensitivity of the *source location estimation* to the spatial search range, size of the sliding window, feature type, and number and combination of sites is also investigated for SCK-CEN ^{41}Ar experiment."

(1.2) Line 60 of section "1. Introduction": "Deterministic assumption"

Deterministic assumptions aim to define the physical feature of source parameters. A typical one is the constant-release assumption, which assumes that the substances are released at a constant rate during the release period (Kovalets et al., 2020, 2018; Efthimiou et al., 2018, 2017; Tomas et al., 2021; Andronopoulos and Kovalets, 2021; Ma et al., 2018). To avoid confusion, we have replaced the terms "Statistical assumption" and "Deterministic assumption" with "*Assumptions on model-observation discrepancies*" and "*Assumptions on the release characteristics*", respectively, in the introduction

section in the revised manuscript.

► Line 38-78 of section "1. Introduction" have been replaced with:

"To reduce the problem of ill-posedness, most previous studies have attempted to constrain the reconstruction by imposing assumptions on *the model-observation discrepancies or release characteristics. Assumptions on model-observation discrepancies* are widely used in Bayesian methods to simultaneously reconstruct the posterior distributions of spatiotemporal source parameters (De Meutter et al., 2021; Meutter and Hoffman, 2020; Xue et al., 2017a). This assumes that the model–observation discrepancies follow a certain statistical distribution (i.e. the likelihood of Bayesian methods), with the normal (Eslinger and Schrom, 2016; Guo et al., 2009; Keats et al., 2007, 2010; Rajaona et al., 2015; Xue et al., 2017a, b; Yee, 2017; Yee et al., 2008; Zhao et al., 2021) and log-normal (Chow et al., 2008; Dumont Le Brazidec et al., 2020; KIM et al., 2011; Monache et al., 2008; Saunier et al., 2019; Senocak, 2010; Senocak et al., 2008) distributions being two popular choices. Other candidates include *t*-distribution (with degrees of freedom ranging from 3 to 10), Cauchy distribution and log-Cauchy distribution, which have been compared with normal and log-normal distributions in reconstructing the source parameters of the Prairie Grass field experiment (Wang et al., 2017). The results demonstrate that the likelihoods are sensitive to both the dataset and the targeted source parameters. Some studies have constructed the likelihood based on multiple metrics that measure the model–observation discrepancies in an attempt to better constrain the solution (Lucas et al., 2017; Jensen et al., 2019). More sophisticated methods involve the use of different statistical distributions for the likelihoods of non-detections and detections (De Meutter et al., 2021; Meutter and Hoffman, 2020). Recent studies have suggested the use of log-based distributions and tailored parameterization of the covariance matrix as a means of better quantifying the uncertainties in the reconstruction (Dumont Le Brazidec et al., 2021). These Bayesian methods have been applied to real atmospheric radionuclide releases, such as the 2017 ^{106}Ru event, and have provided important insights into the source and release process (Dumont Le Brazidec et al., 2020; Saunier et al., 2019; Dumont Le Brazidec et al., 2021; De Meutter et al., 2021). However, these studies have also revealed that the likelihood in Bayesian methods must be exquisitely designed and parameterized to achieve satisfactory spatiotemporal source reconstruction (Dumont Le Brazidec et al., 2021; Wang et al., 2017). With suboptimal design, the reconstruction may exhibit a bimodal posterior distribution (Meutter and Hoffman, 2020), which remains a challenge for robust applications in different scenarios.

Assumptions on the release characteristics aim to reduce the dimension of the solution space to 4 or 5, i.e. the two source location coordinates, the total release, and the release time (or the release start and end time), by assuming that the substances are released instantaneously at a release time (or constantly during a release time period) (Kovalets et al., 2020, 2018; Efthimiou et al., 2018, 2017; Tomas et al., 2021; Andronopoulos and Kovalets, 2021; Ma et al., 2018). Under these assumptions, the correlation-based method has exhibited high accuracy for ideal cases under stationary meteorological conditions, such as synthetic simulation experiments (Ma et al., 2018) and wind tunnel experiments (Kovalets et al., 2018; Efthimiou et al., 2017). However, previous studies have also demonstrated that the application in real-world cases may be much more challenging, (Kovalets et al., 2020; Tomas et al., 2021; Andronopoulos and Kovalets, 2021; Becker et al., 2007), because the release usually exhibits temporal variations and may experience non-stationary meteorological fields. The interaction between the time-varying release characteristics and non-stationary meteorological fields is ignored in the instantaneous-release and constant-release assumption, leading to inaccurate reconstruction."

(1.3) Line 108 of section "2.1 Source reconstruction models": "$\mathbf{A}(\mathbf{r}) = [\boldsymbol{A}_1(\mathbf{r}), \boldsymbol{A}_2(\mathbf{r}), \cdots, \boldsymbol{A}_N(\mathbf{r})]^T \in \mathbb{R}^{N \times N}$"

The matrix $\mathbf{A}(\mathbf{r})$ is not a square matrix in general. We have modified the dimension of the matrix: $\mathbf{A}(\mathbf{r}) =$

$[A_1(\mathbf{r}), A_2(\mathbf{r}), \cdots, A_N(\mathbf{r})]^T \in \mathbb{R}^{N\times S}$, where N is the number of sequential time steps and S is the length of release rate vector $\mathbf{q}$.

► Line 100-109 of section "2.1 Source reconstruction models" have been replaced with:

"For an atmospheric radionuclide release, Eq. (1) relates the observations at each observation site to the source parameters:

$$\boldsymbol{\mu} = \mathbf{F}(\mathbf{r}, \mathbf{q}) + \boldsymbol{\varepsilon}\,, \tag{1}$$

where $\boldsymbol{\mu} = [\mu_1, \mu_2, \cdots, \mu_N] \in \mathbb{R}^N$ is an observation vector composed of observations at N sequential time steps, the function $\mathbf{F}$ maps the source parameters to the observations, i.e. an atmospheric dispersion model, $\mathbf{r}$ refers to the source location, $\boldsymbol{q} \in \mathbb{R}^S$ is the temporally varying release rate, and $\boldsymbol{\varepsilon} \in \mathbb{R}^N$ is a vector containing both model and measurement errors.

In most source reconstruction models, $\mathbf{F}$ is simplified to the product of $\mathbf{q}$ and a source–receptor matrix $\mathbf{A}$ that depends on the source location:

$$\boldsymbol{\mu} = \mathbf{A}(\mathbf{r})\mathbf{q} + \boldsymbol{\varepsilon}\,, \tag{2}$$

where $\boldsymbol{A(r)} = [A_1(\boldsymbol{r}), A_2(\boldsymbol{r}), \cdots, A_N(\boldsymbol{r})]^T \in \mathbb{R}^{N\times S}$ and each row describes the sensitivity of an observation to the release rate $\mathbf{q}$ given the source location $\mathbf{r}$."

(1.4) Line 131 of section "2.2 Spatiotemporal decoupling": "sliding window"

As outlined in Eq. (4), a one-sided window is employed. This one-sided temporal sliding-window average filter involves the current and previous observations in the window, acknowledging that future observations are not available for filtering in practice. Compared to the centered window, the one-sided window excels in real-time data processing and rapid response to changes in the observations, making it more suitable for real applications.

► Line 128-132 of section "2.2 Spatiotemporal decoupling" have been replaced with:

"In this study, the following operator matrix is constructed to impose a *one-sided* temporal sliding-window average filter (Eamonn Keogh, Selina Chu, 2004):

$$\mathbf{P} = \frac{1}{T}\begin{bmatrix} 1 & & & & & & & & & \\ 1 & 1 & & & & & & & & \\ & \vdots & & & & & & & & \\ 1 & 1 & \cdots & 1 & & & & & & \\ 1 & 1 & \cdots & 1 & 1 & & & & & \\ & 1 & 1 & \cdots & 1 & 1 & & & & \\ & & 1 & 1 & \cdots & 1 & 1 & & & \\ & & & \ddots & \ddots & \ddots & \ddots & \ddots & & \\ & & & & 1 & 1 & \cdots & 1 & 1 & \\ & & & & & 1 & 1 & 1 & 1 & 1 \end{bmatrix}, \tag{4}$$

where T is the size of the sliding window. *This one-sided filter involves the current and previous observations in the window, acknowledging that future observations are not available for filtering in practice.* Although a sliding-window average filter is used in this study, Eq. (3) is compatible with more advanced processing methods."

(1.5) Line 228 of section "2.6.2 Simulation settings of atmospheric dispersion model": "sample"

This term refers to an individual simulation using one of the candidate source locations. Therefore, each "sample" represents a simulated dispersion scenario with a different candidate source location. To clarify this point, we have replaced the term "sample" with "simulation" in the revised manuscript and explained the meaning of "sample".

► Line 228-230 of section "2.6.2 Simulation settings of atmospheric dispersion model" have been replaced with:

"To establish the datasets for the XGBoost model, *2000 simulations and 1000 simulations with different source locations*

were performed by RIMPUFF for Oct. 3 and Oct. 4, respectively. The *candidate* source locations were *randomly* sampled from the shaded zones in Fig. 2a, which were determined according to the positions of the observation sites and the upwind direction. *Each simulation, along with its corresponding source location, forms one sample.*"

(2) Presentation of the machine learning method:

We have added descriptions to the figure caption of the Fig. 1 and relabeled the root nodes using yellow squares in Fig. 1, providing a more accurate and detailed introduction to the decision tree model. To avoid confusion, we have replaced the symbol "*T*" with "*M*" in Eq. (7) and have provided additional descriptions for all the parameters.

► Line 147-157 of section "2.3 Source localization without knowing the exact release rates" have been replaced with: "where K is the number of trees, $\mathcal{F} = \{f(x) = \boldsymbol{\omega}_{Q(x)}\}(Q: \mathbb{R}^p \to M, \boldsymbol{\omega} \in \mathbb{R}^M)$ is the space of decision trees, and Q represents the structure of each tree, mapping the feature vector to M leaf nodes. Each f_k corresponds to an independent tree structure Q with leaf node weight $\boldsymbol{\omega} = (\omega_1, \omega_2, \cdots, \omega_M)$. Equation (5) is then used to predict $\hat{\mathbf{r}}_i = (\hat{x}_i, \hat{y}_i)$ for the i-th sample.

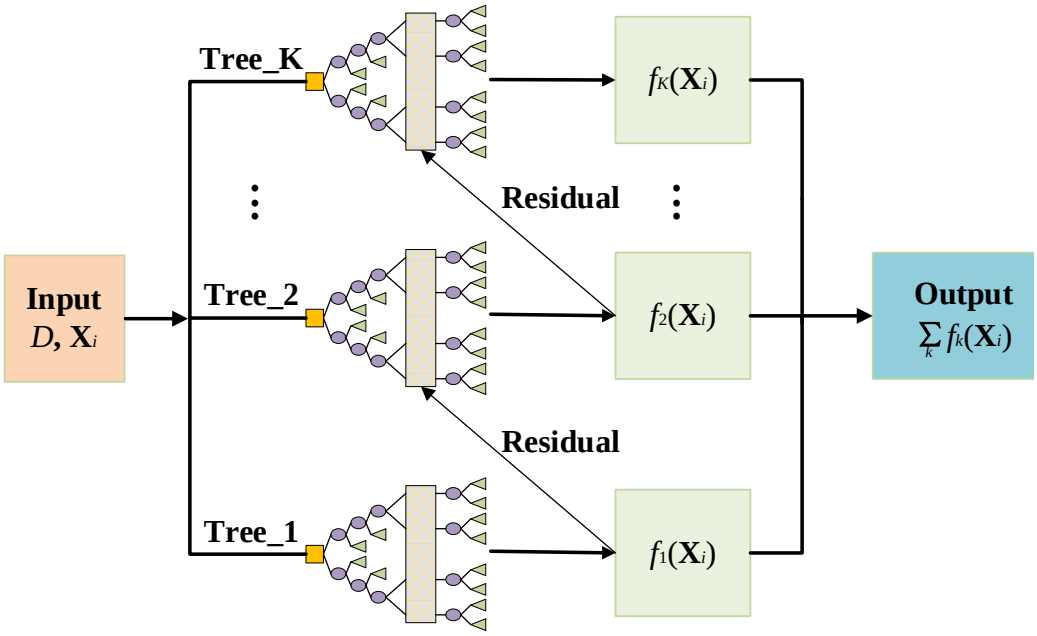

Figure 1. Flowchart of XGBoost for predicting $\hat{\mathbf{r}}_i$ based on decision tree model. *The yellow squares are the root nodes within each tree, representing the input features in this paper. The purple ellipses denote the child nodes where the model evaluates input features and make decisions to split the data. The green rectangles depict the leaf nodes and refer to the prediction results. The vertical rectangles abstract the internal splitting processes of the trees, indicating decision-making not explicitly detailed in the diagram.*

XGBoost trains $G(\mathbf{X})$ in Eq. (5) by continuously fitting the residual error until the following objective function is minimized:

$$Obj^{(t)} = \sum_{i=1}^{n} \left(\mathbf{r}_i - \left(\hat{\mathbf{r}}_i^{(t-1)} + f_t(\mathbf{X}_i)\right)\right)^2 + \sum_{i=1}^{t} \Omega(f_i)\,, \tag{6}$$

where t represents the training of the t-th tree and $\Omega(f_i)$ is the regularization term, given by:

$$\Omega(f) = \Upsilon M + \frac{1}{2}\lambda \sum_{j=1}^{M} \omega_j^2\,, \tag{7}$$

where M is the number of leaf nodes, ω_j is the leaf node weight for the j-th leaf node, Υ and λ are penalty coefficients. The minimization of Eq. (6) provides the parametric model $G(\mathbf{X})$ that maps the feature ensemble $\mathbf{X}$ extracted from $\boldsymbol{\mu}_p$ to the source location $\mathbf{r}$."

(3) Dispersion model error considerations:

We agree with your point regarding the impact of dispersion model errors. To address this issue, we will add an in-depth analysis of the dispersion model errors and their influences on our source reconstruction. Perturbation will be added to the input parameters (such as the wind speed and atmospheric stability) of atmospheric dispersion simulations, to simulate the potential dispersion model error. The proposed method will use these perturbed simulations to train the XGBoost model and to reconstruct the source. The error statistics of the reconstructed source will be discussed both qualitatively and quantitatively. Because these simulations are time-consuming, we will provide the results in the revised manuscript.

(4) The testing of the method:

To address your concern, we have added another validation based on the first release of the European Tracer Experiment (ETEX-1) (Nodop et al., 1998), which is continental scale. We have provided an overview of the ETEX-1 experiment and source reconstruction results below. Detailed results and discussions have been included in the revised manuscript.

2.6 Multi-scale Validations

2.6.1 Field experiments

The ETEX-1 experiment took place at Monterfil in Brittany, France, on 23 October 1994 (Nodop et al., 1998). During ETEX-1, a total release of 340 kg of PMCH was released into the atmosphere during 23 Oct 1994 16:00:00 UTC and 24 Oct 1994 03:50:00 UTC. As illustrated in Fig. 2b, the source coordinates were (2.0083°W, 48.058°N). A total of 3104 available observations (3h-averaged concentrations) were collected by 168 sites. ETEX-1 has been commonly used as a validation scenario for reconstructing atmospheric radionuclide releases (Ulimoen and Klein, 2023; Tomas et al., 2021). The candidate source locations are uniformly sampled from the green shaded zone. We choose two groups of observation sites: the first comprises four sites (i.e. B05, D10, D16, F02) randomly selected from the sites within the sample zone (Group1, with a total of 92 available observations), and the second involves four sites (i.e. CR02, D15, DK08, S09) randomly selected from the sites beyond the sample zone boundaries (Group2, with a total of 90 available observations). Compared to the SCK-CEN ^{41}Ar experiment, the observations of the ETEX-1 exhibit temporal sparsity, lower temporal resolution, and increased complexity in meteorological conditions.

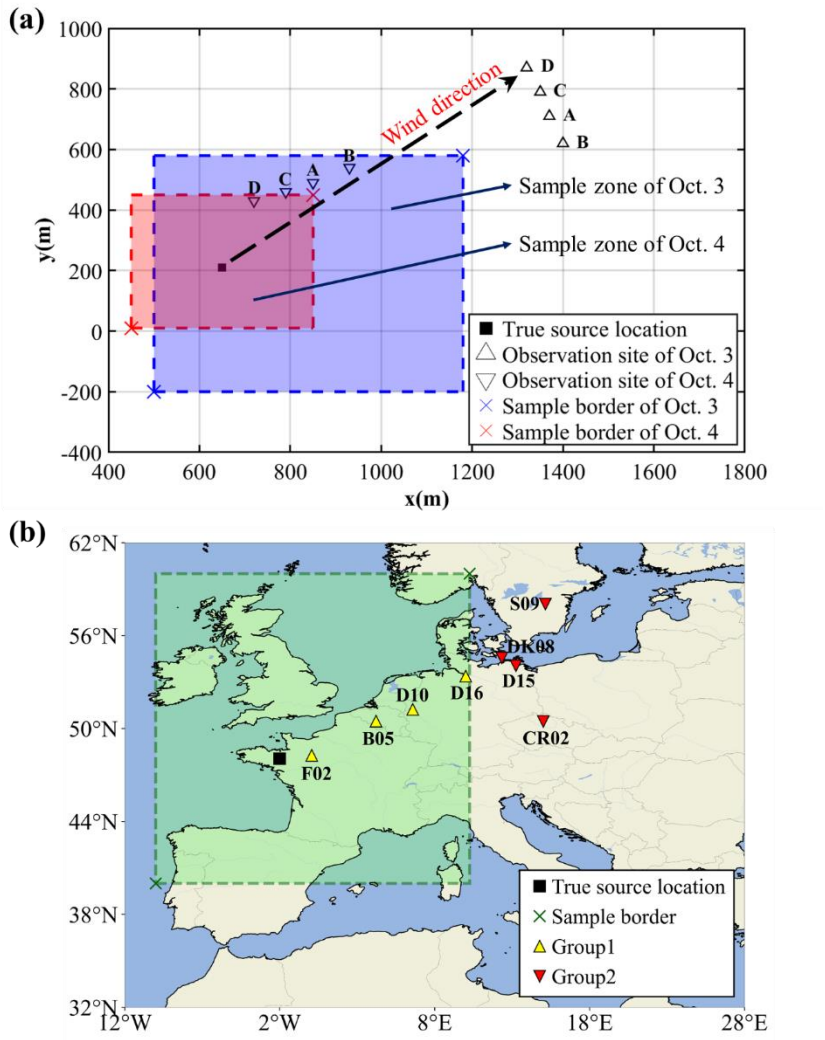

Figure 2. Release location and observation sites of two filed experiments. (a) SCK-CEN ^{41}Ar experiment. The map was created based on the relative positions of the release source and observation sites, as detailed in (Drews et al., 2002). The coordinate of the sample border is (500m, -200m) and (1180m, 580m) on Oct. 3, and (450m, 10m) and (850m, 450m) on Oct. 4. It was plotted using MATLAB 2016b, instead of created by a map provider; (b) ETEX-1 experiment. The map was created based on the real longitudes and latitudes of the release source and observation sites, as detailed in (Nodop et al., 1998). The coordinate of the sample border is (10°W, 40°N) and (10°E, 60°N). It was plotted using the function *cartopy* of Python, instead of created by a map provider.

2.6.2 Simulation settings of atmospheric dispersion model

For the ETEX-1 experiment, the FLEXible PARTicle (FLEXPART) model (version 10.4) was applied to simulate the dispersion of PMCH (Pisso et al., 2019). The meteorological data were from the United States National Centers of Environmental Prediction Climate Forecast System Reanalysis, which has a spatial resolution of 0.5°×0.5° and time resolution of 6h. To rapidly establish the relationship between the varying source locations and the observations, 182 backward simulations were performed using FLEXPART. The candidate source locations were uniformly sampled from the shaded zone in Fig. 2b, resulting a total of 6561 source locations. As described in Sect. 2.5.1, 2624 candidate source locations are preserved by pre-screening step. The constant factors mentioned in Sect. 2.5.2 are 5.60×10^{12} and 2.86×10^{13}.

3.2 Optimization of XGBoost model

3.2.2 Feature selection

Figure 4 compares the importance of the selected features at each site. For the ETEX-1 experiment, Fig. 4c and d

showed that the features of Group1 and Group2 are almost reserved after the feature selection process (only one feature is removed for each case), indicating fewer redundant features than that in the SCK-CEN ^{41}Ar experiment. The time-domain features are also dominant, but the frequency-domain features at some sites also play important roles such as D16 and S09. The MCVs of the ETEX-1 experiment have similar variation trend as that of the SCK-CEN ^{41}Ar experiment (Fig. S4c and d). However, the Group1 has obviously lower MCV than other experiments.

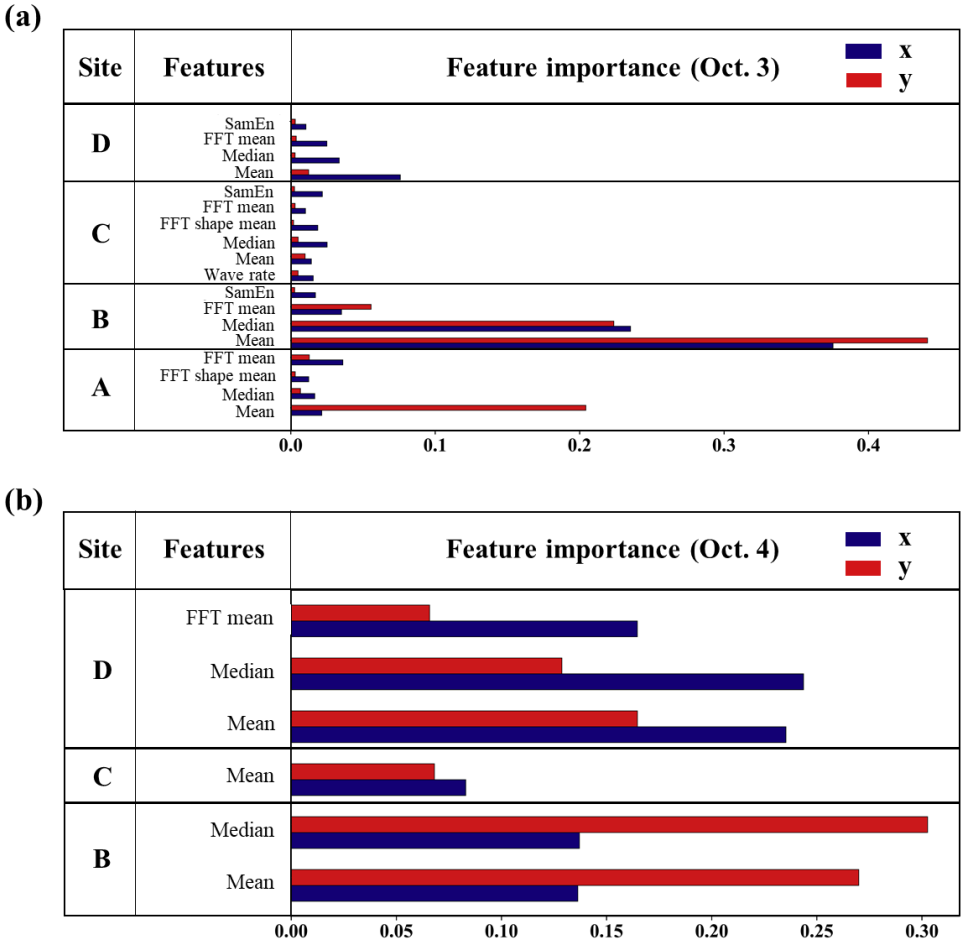

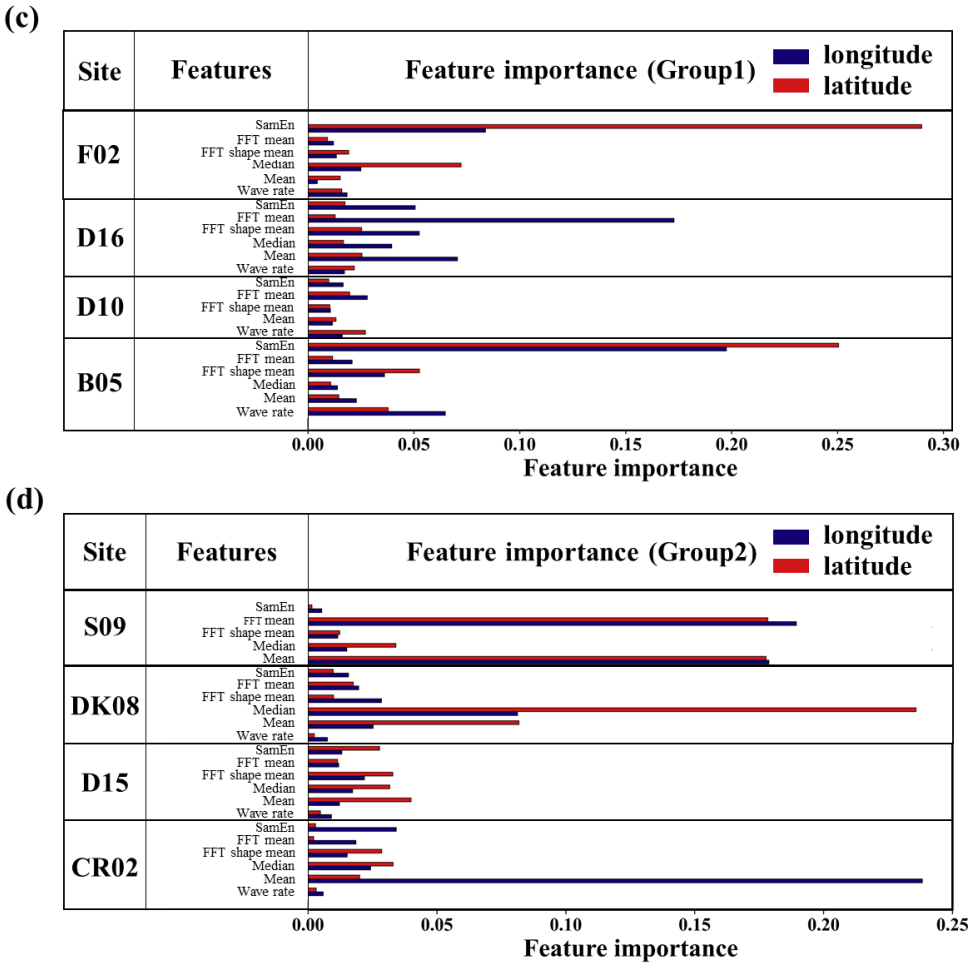

Figure 4. Feature importance. (a) Oct. 3; (b) Oct. 4; (c) Group1; (d) Group2.

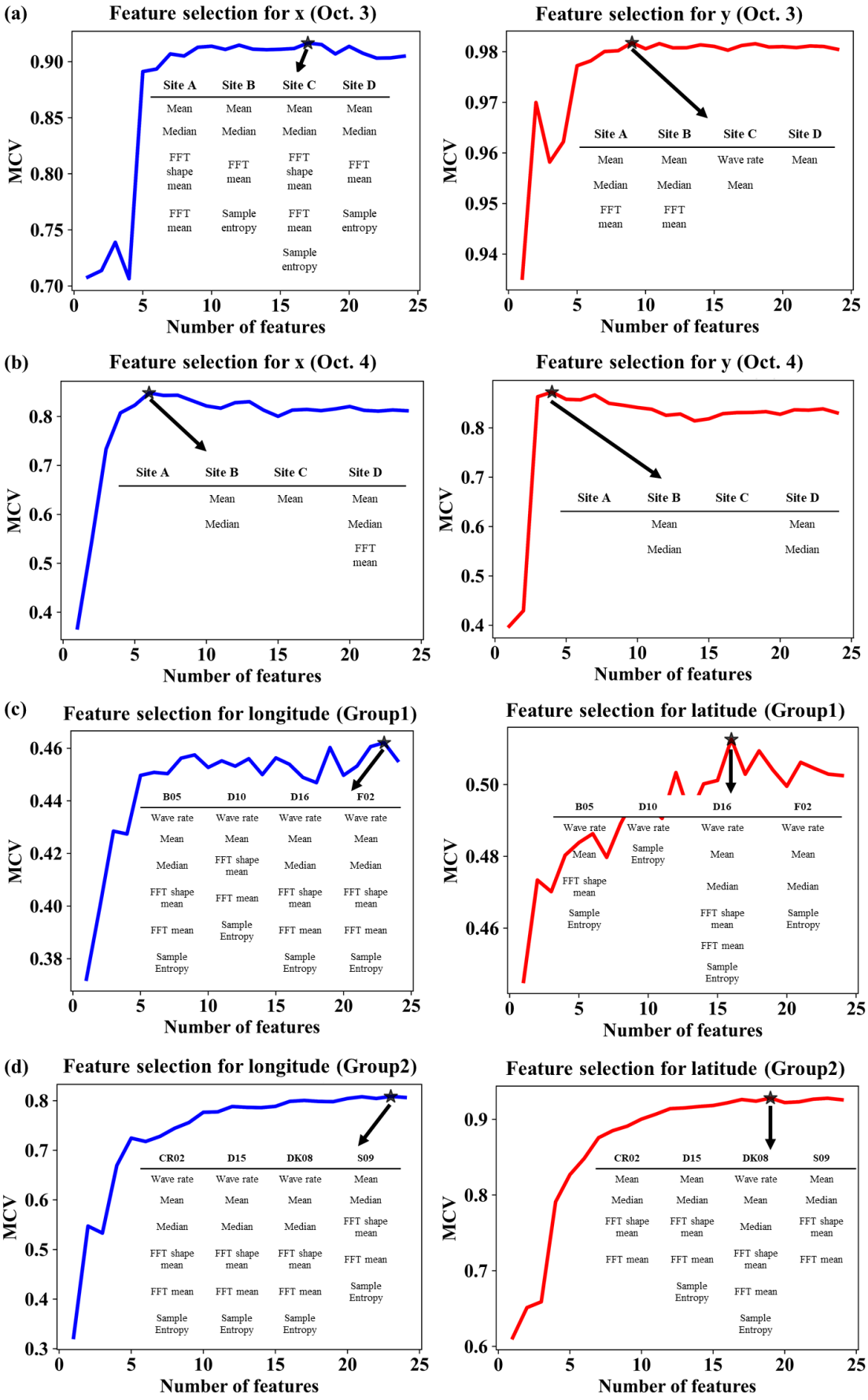

Figure S4. Results of feature selection in x (longitude) and y (latitude) directions. (a) Oct. 3; (b) Oct. 4; (c) Group1; (d) Group2. The black stars denote the optimal number of features. The table inserted in each subgraph lists the selected features for each observation site.

3.3 Source reconstruction

3.3.1 Source location estimation

Figure 5 compares the best-estimated source locations of the correlation-based method, the Bayesian method, and the proposed method with the ground truth. For the ETEX-1 experiment, the pre-screening zone also covers the true source location for Group1 and Group2. But source locations estimated by the correlation-based method are 411.85 km and 486.41 km away from the ground truth for Group1 and Group2, respectively. The location error of the Bayesian method estimates is only 30.50 km for Group1, but it increases to 520.77 km for Group2, indicating its sensitivity to the observations. In contrary, the proposed method achieves the lowest source location errors, which are below 10 km and 20 km for Group1 and Group2, respectively. Because the feature selection hardly removed the features (Fig. 4c and d), the estimated source locations with and without feature selection basically overlap for both groups.

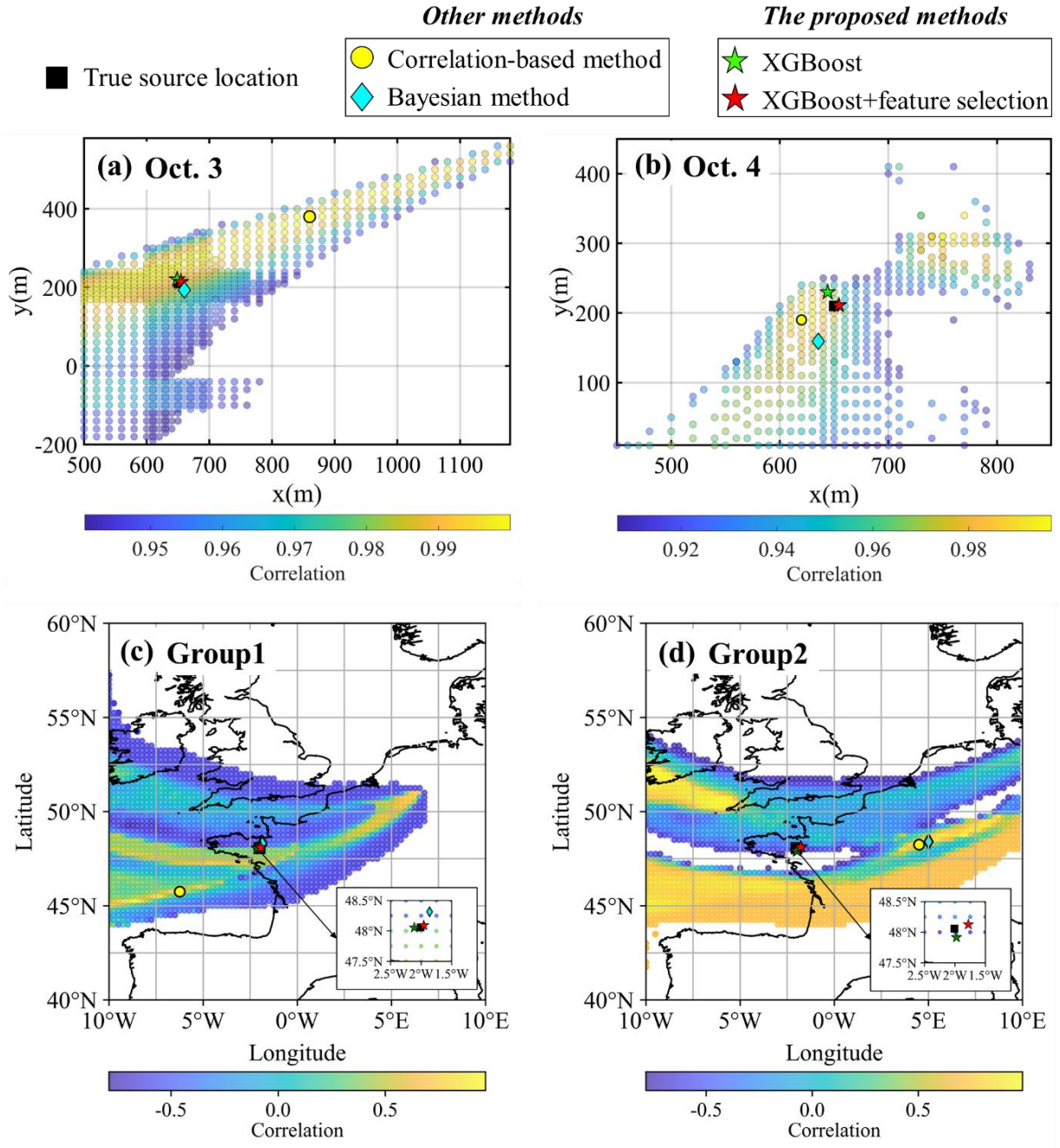

Figure 5. Source location estimation results. The yellow dots denote the maximum correlation points, which are the localization results of the correlation-based method. The green and red stars represent the localization results based on

XGBoost before and after feature selection, respectively. The cyan diamonds represent the localization results based on the Bayesian method. (a) Oct. 3; (b) Oct. 4; (c) Group1; (d) Group2. A detailed enlargement of the region around (2.5°W, 47.5°N) to (1.5°W, 48.5°N) is shown in the bottom right corner in (c) and (d) to highlight the source location estimation results of the proposed methods.

3.3.2 Release rates

Figure 6 displays the release rates estimated by the Bayesian and PAMILT methods based on the source location estimates in Fig. 5. For the two ETEX-1 groups (Fig. 6c and d), Bayesian estimates exhibit noticeable fluctuations, leading to underestimations–58.11% for Group1 and 51.44% for Group2. Furthermore, the temporal profile of the Bayesian estimates for Group2 completely falls out of the true release window. In contrast, most releases of the PAMILT estimates are within the true release time window, especially for Group2, despite overestimations reach 52.38% for Group1 and 57.65% for Group2, after feature selection process. Compared to the SCK-CEN ^{41}Ar experiment, the increased deviation in the ETEX-1 experiment may be attributed to the limited observations at the four sites as shown in Fig. S3.

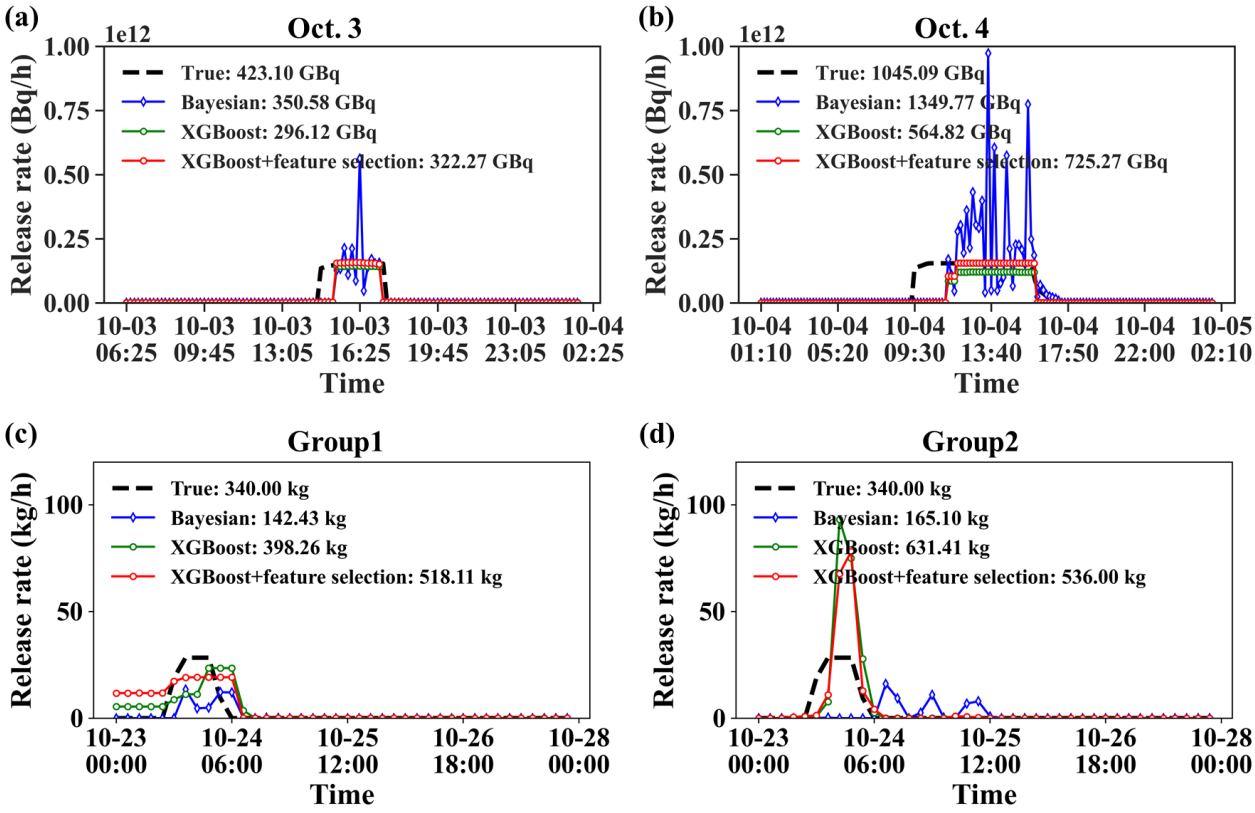

Figure 6. Release rate estimation results with different location estimates. (a) Oct. 3; (b) Oct. 4; (c) Group1; (d) Group2. The release rates labelled by XGBoost or XGBoost+feature selection are estimated using PAMILT method.

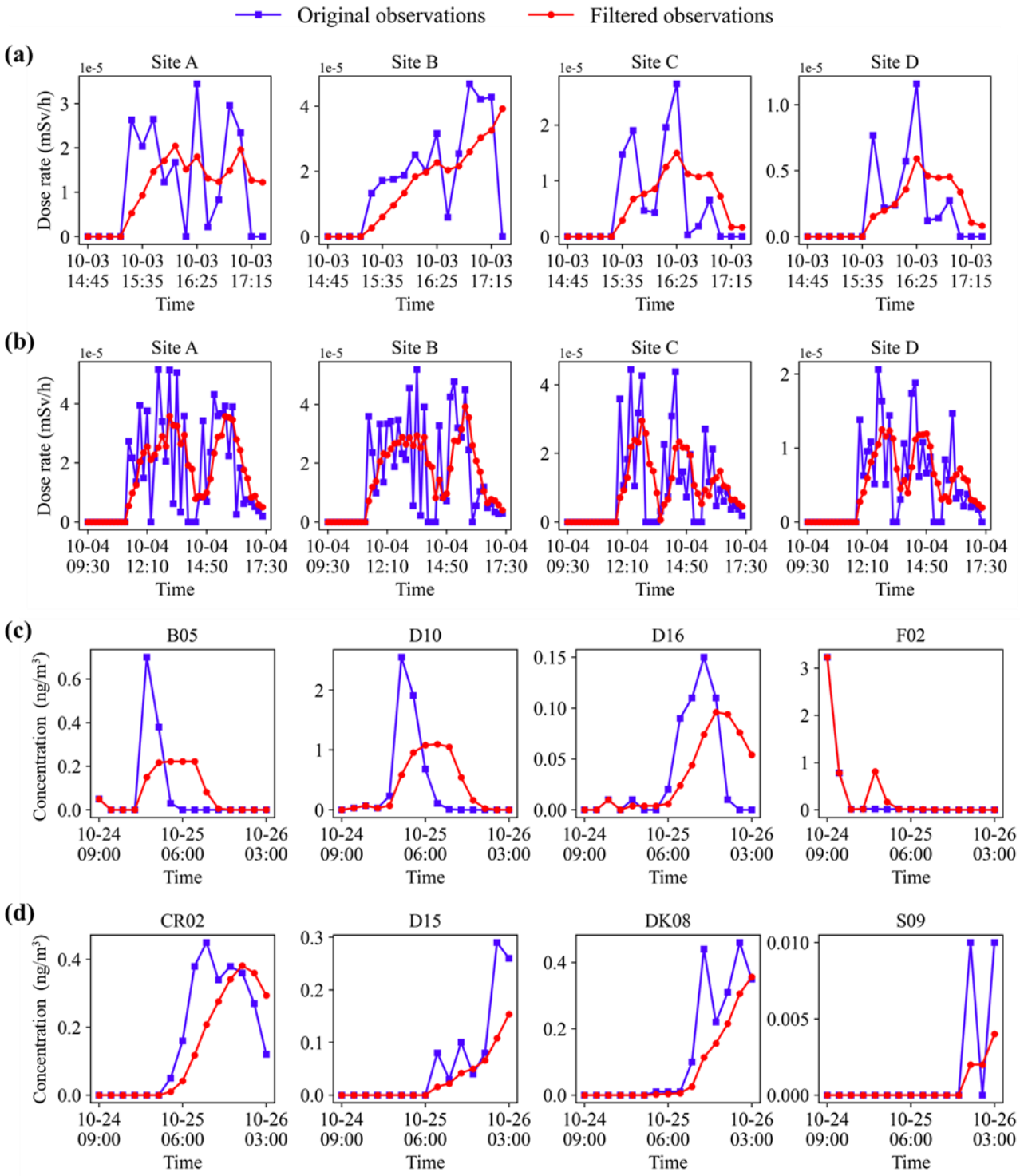

Figure S3. Observations before and after filtering at observation sites. (a) Oct. 3; (b) Oct. 4; (c) Group1; (d) Group2.

3.3.3 Uncertainty range

Figure 7 compares the spatial distribution of 50 estimates produced by the different source location estimation methods. For the ETEX-1 experiment, the estimates of the correlation-based method are quite spread, whereas those of the Bayesian method are more concentrated. The Bayesian estimates are close to the truth in Group1, but are noticeably deviated in Group2. The phenomenon indicates that the Bayesian method is sensitive to the observations, especially when observations are limited. Fig. S5c and d also reveals that the Bayesian-estimated posterior distribution is multimodal for both ETEX-1 groups, which can be avoided by using additional observations (Fig. S5e). In contrast, the

proposed method provides estimates quite concentrated around the truth for both Group1 and Group2, indicating its efficiency in the case of limited observations. Compared to Group2, Group1 exhibits lower source location error. This is attributed to the fact that, as shown in Fig. 2, Group1's four observation sites are situated closer to the sampled source locations than those of Group2, thereby providing more accurate plume characteristics and resulting in lower dispersion error.

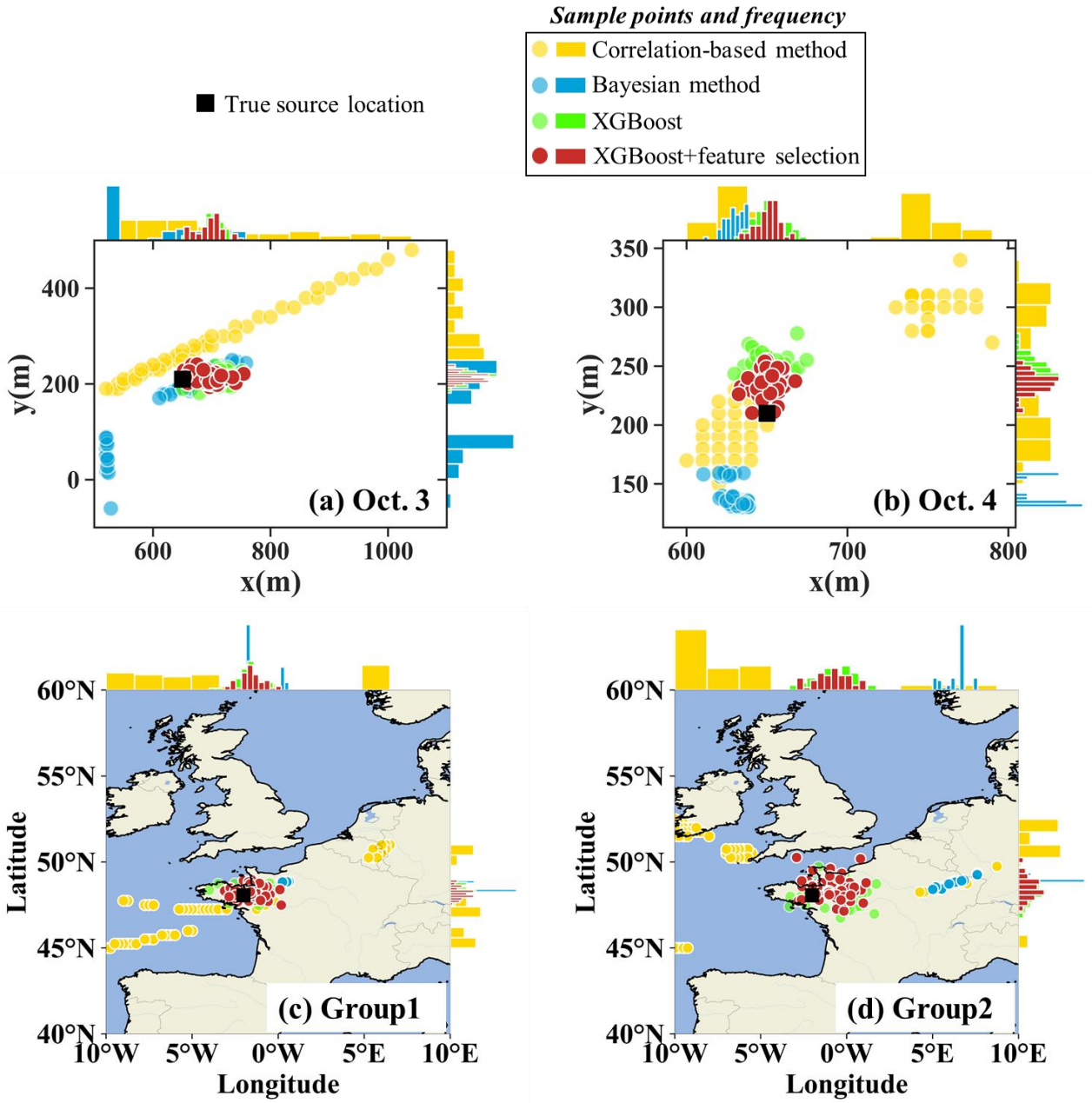

Figure 7. Distribution of source location estimation results over 50 calculations. (a) Oct. 3; (b) Oct. 4; (c) Group1; (d) Group2.

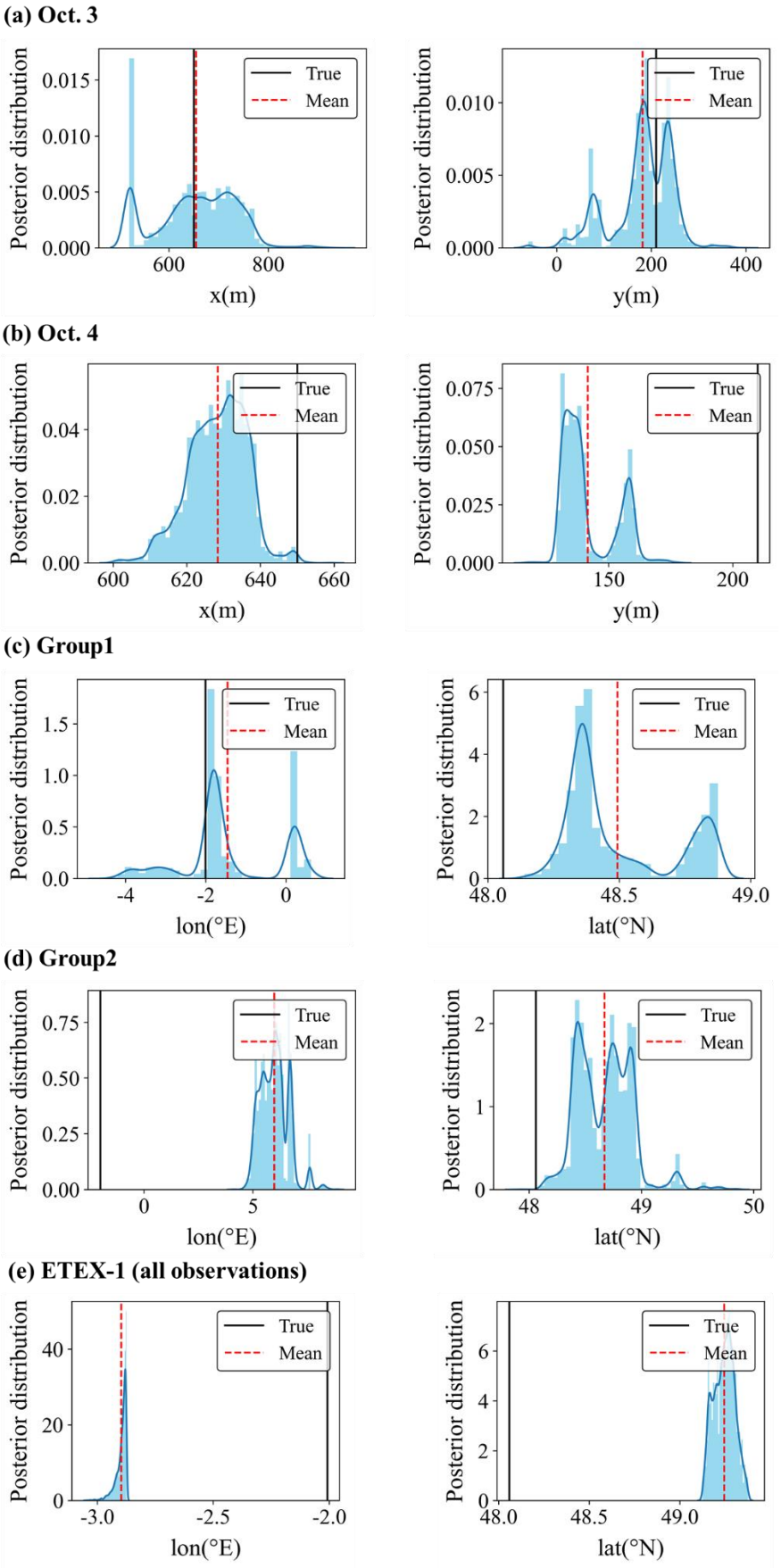

Figure S5. Posterior distributions of source location parameters. (a) Oct. 3; (b) Oct. 4; (c) Group1; (d) Group2; (e) ETEX-1 (all observations in ETEX-1 are used). The black solid lines denote the true location parameters and the dashed lines denote the mean estimates of all posterior samples.

Figure 9 compares the uncertainty ranges of the release rate estimates in the two ETEX-1 groups. For both groups, the Bayesian estimates show underestimations (including the mean estimate), but it presents small uncertainty range (Fig. 9a and c). In addition, the Bayesian estimates all fall out of the time window of the true release in Group2 (Fig.9c). The mean PAMILT estimates are more accurate mean Bayesian estimates, which most releases are within the time window of the true release (Fig. 9b and d). However, PAMILT estimates for the ETEX-1 experiment show a large uncertainty range in both groups, in contrast to the SCK-CEN ^{41}Ar experiment. The reason for this discrepancy is that the source-receptor matrices of the ETEX-1 experiment are more sensitive to errors in source location than those of the SCK-CEN ^{41}Ar experiment. The greater sensitivity originates from the ETEX-1 experiment's more complex meteorological conditions, both spatially and temporally. As for the mean total release, the Bayesian method shows underestimations of 70.93% for Group1 and 74.15% for Group2. In comparison, the proposed method shows deviation of only 0.71% for Group1 and 0.09% for Group2, after feature selection.

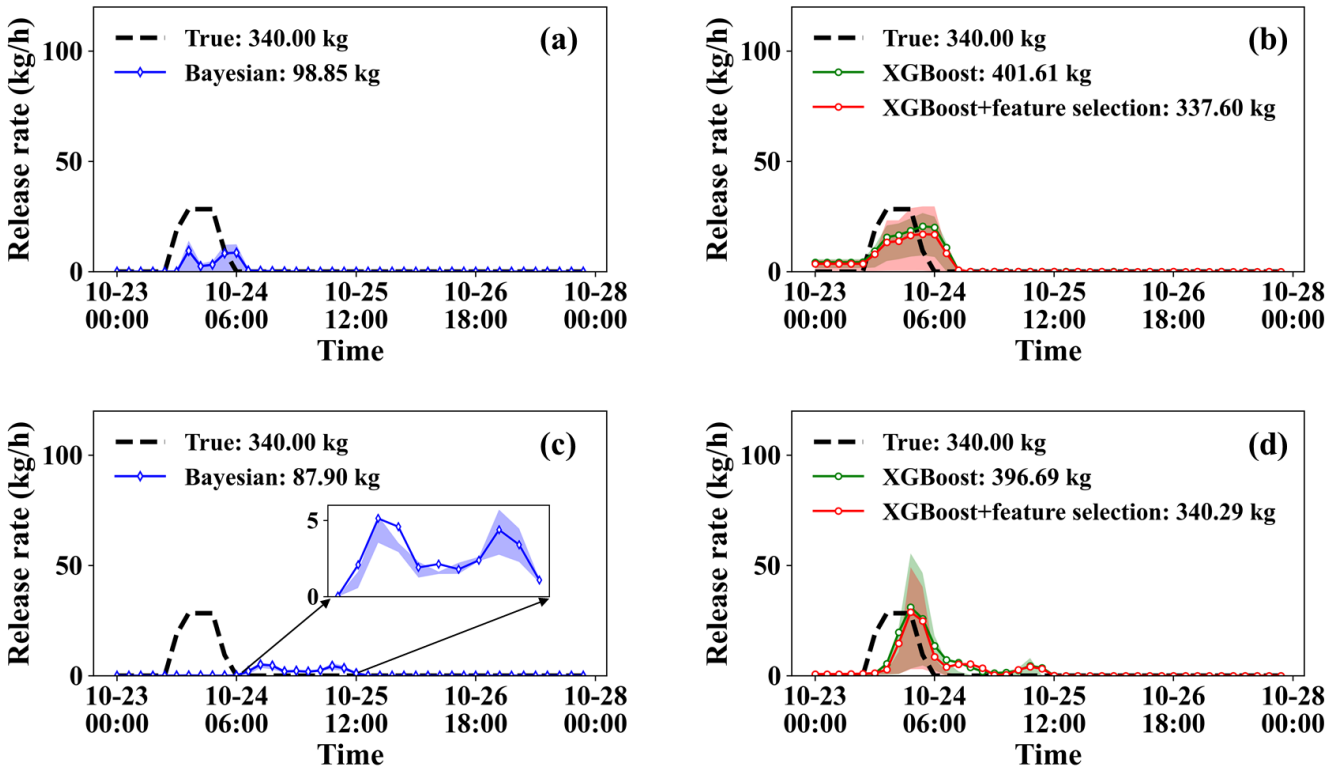

Figure 9. Release rate estimates over 50 calculations in ETEX-1 experiment. (a) Group1-Bayesian method; (b) Group1-PAMILT method; (c) Group2-Bayesian method; (d) Group2-PAMILT method.

Table 3 lists the mean and standard deviation of the relative errors for the 50 estimates given by different methods. For the ETEX-1 experiment, the Bayesian method shows case-sensitive performances with respect to the mean relative error of source location estimation, whereas the proposed method gives the most accurate source locations with small uncertainties for both groups. As for the total release, the proposed methods show smaller mean relative errors than the Bayesian methods, but the Bayesian method shows a smaller standard deviation.

Table 3. Relative errors of source reconstruction. $\delta_{\mathbf{r}}$ represents the relative error of source location, which is positive and δ_Q denotes the relative error of total release, where a positive value indicates overestimation and a negative value denotes underestimation.

Experiments	Statistical parameters (Relative error)		Correlation-based method	Bayesian method	The proposed method	
					XGBoost	XGBoost+ feature selection
Oct. 3	$\delta_{\mathbf{r}}$	Mean	14.10%	11.88%	5.18%	4.68%
		Std	11.37%	7.53%	1.79%	2.05%
	δ_Q	Mean	-	153.61%	-16.93%	-18.30%
		Std	-	189.76%	9.45%	8.01%
Oct. 4	$\delta_{\mathbf{r}}$	Mean	14.30%	12.83%	6.83%	4.71%
		Std	9.60%	1.68%	1.76%	1.53%
	δ_Q	Mean	-	42.29%	-54.12%	-47.42%
		Std	-	15.05%	6.47%	5.85%
Group1	$\delta_{\mathbf{r}}$	Mean	16.95%	3.22%	2.32%	2.42%
		Std	7.46%	2.75%	1.43%	1.43%
	δ_Q	Mean	-	-70.93%	18.12%	-0.71%
		Std	-	17.87%	99.85%	102.01%
Group2	$\delta_{\mathbf{r}}$	Mean	21.9%	23.97%	5.21%	4.97%
		Std	5.05%	1.97%	2.42%	2.35%
	δ_Q	Mean	-	-74.15%	16.67%	0.09%
		Std	-	11.68%	93.50%	109.56%

Major points

Comment#1:

Title: Both “Generalized” and “Spatiotemporally-decoupled” are not accurately reflecting the current two-step method. The word “non-constant” in the title does not sound appropriate either. In reality, there are rarely constant releases. The author should reconsider the title.

Response to comment#1:

Thank you very much for the comment on the title. We have deleted the "non-constant" and “Generalized” in the title and have replaced the term “Spatiotemporally-decoupled” with “*Spatiotemporally-separated*”, to more accurately reflect the essence of the two-step method described in the manuscript. The revised title now reads: “*A spatiotemporally-separated framework for reconstructing the source of atmospheric radionuclide releases.*”

Comment#2:

Abstract, lines 12-14: This statement is not accurate. The temporal variation of the release rates may be reflected on the plume shape, not only on the temporal variations of the observations. In theory, some problems cannot be decoupled. So the proposed method cannot be a real general framework. The limitation of the method has to be pointed out in the paper.

Response to comment#2:

(1) Regarding the influence of the temporal variation of the release rates:

We agree that the temporal variation of release rates influence the plume shape. This influence may be difficult to capture using only a limited number of observation sites, which is the case of SCK-CEN ^{41}Ar experiment. For this reason, we focus on reducing the influence of temporal variations in the release rate on the observations, whereas the influence on the plume shape is not directly considered. However, our future efforts will be directed towards integrating spatial features to further enhance the method. The limitation and the future efforts have been pointed out in the section “4. Conclusions” after Line 475:

“*However, the proposed method does not consider the influence of temporal variations of the release rate on the plume shape. Our future efforts will be directed towards integrating spatial features to further enhance the method.*”

(2) Concerning whether the proposed method is truly a general framework:

You raised an essential point about theoretical constraints where some problems cannot be decoupled. For these problems, our goal is to minimize the influence of temporal variations in the release rate on the observations, so that we can achieve spatiotemporally-separated reconstruction. To eliminate ambiguity, we have restated the characteristics of the proposed method, using the term “*spatiotemporally-separated*” rather than “spatiotemporally-decoupled” in the revised manuscript. Furthermore, to verify the applicability of the proposed method, we have also validated it using another field experiment at a different spatial scale, which have been presented in the responses to the **General comments**. This will help readers better understand the limitations and superiority of the proposed method and encourage further researches to overcome the constraints. Followed by comment#1 and comment#2, we have revised the abstract to ensure that it accurately reflects the updated focus of our study. Additionally, several relevant titles have been updated to ensure consistency with these modifications.

► Line 9-14 of section “Abstract” have been replaced with:

“Determining the source location and release rate are critical in assessing the environmental consequences of atmospheric radionuclide releases, but remain challenging because of the huge multi-dimensional solution space. We

propose a *spatiotemporally-separated* two-step framework to reduce the dimension of the solution space in each step and improves the *source* reconstruction accuracy of *radionuclide* releases. The *separating* process is conducted by applying a temporal sliding-window average filter to the observations, thereby reducing the influence of temporal variations in the release rate *on the observations* and ensuring that the features of the filtered data are dominated by the source location."

► Title "2.2 Spatiotemporal decoupling" in line 110 has been replaced with:

"2.2 *Observation filtering for spatiotemporally-separated reconstruction*"

► Title "2.8.1 Decoupling" in line 255 has been replaced with:

"2.8.1 *Observation filtering*"

► Title "3.1 Decoupling performance" in line 291 has been replaced with:

"3.1 *Filtering performance*"

Comment#3:

Abstract, line 15: Locating a source location is not "localization". This needs to be corrected throughout the paper.

Response to comment#3:

We appreciate your comment on the use of the term "localization". We have replaced the relevant descriptions with "source location estimation", which may precisely describe the process in our research. Accordingly, we have diligently revised the term throughout the paper to ensure accuracy and consistency. For example,

► Line 15 of section "Abstract" has been replaced with:

"A machine learning model is trained to link these features to the source location, enabling independent *source location estimation*."

► Line 94-97 of section "1. Introduction" has been replaced with:

"The performance of the proposed method is compared with the correlation-based method for *source location estimation* and the Bayesian method for spatiotemporal accuracy. The sensitivity of the *source location estimation* to the spatial search range, size of the sliding window, feature type, and number and combination of sites is also investigated for SCK-CEN ^{41}Ar experiment."

Comment#4:

Abstract, line 18: A relative error of about 50% for the Oct. 4 total release is probably not deemed "accurate". It is better to present the results more objectively with the actual number listed in Table 3.

Response to comment#4:

Thank you for your valuable feedback. In light of your suggestion, we have modified the abstract to more objectively reflect the results.

► Line 16-19 of section "Abstract" has been changed from:

"Validation using SCK-CEN ^{41}Ar experimental data demonstrates that the localization error is less than 1%, and the temporal variations, peak release rate, and total release are reconstructed accurately. The proposed method exhibits higher accuracy and a smaller uncertainty range than the correlation-based and Bayesian methods."

to:

"*In applying the method to the SCK-CEN ^{41}Ar experiment, the lowest relative source location errors are only 0.60% and 0.80% for Oct. 3 and Oct. 4, respectively. The proposed method demonstrates higher accuracy and a smaller uncertainty range than the correlation-based and Bayesian methods in estimating source location. Regarding release rate estimation,*

the temporal variations are accurately reconstructed. Compared to the Bayesian method, the mean total release estimate is improved, showing an average 65.09% reduction in relative error."

Comment#5:

Line 94: The authors seem to suggest that the correlation-based method only applies when constant-release assumption is made. This is not accurate. Constant release is only one assumption that reduces the complexity of the problem. If the release starting time or duration is not known. Such assumption may not be enough to guarantee a unique solution of the source location. On the other hand, if a source is not constant, but the release time period and temporal profile are known, it is probably easy to get the source location even without the constant-release assumption.

Response to comment#5:

We agree with you that constant release is only one assumption that reduces the complexity of the problem and our descriptions need to be improved. To avoid confusion, we have deleted the term "(constant-release assumption)" in Line 94 in the revised manuscript. In the introduction section, we have emphasized that: the constant-release assumption may lead to inaccurate source location estimation, such as the case of the correlation-based method, because the constant-release assumption ignores the interaction between the time-varying release characteristics and non-stationary meteorological fields. We also agree that the source location can easily be estimated, if the release time period and temporal profile are known, even without the constant-release assumption. We did not mention this scenario, because this is not the focus of our study. Instead, we mainly consider atmospheric radionuclide releases where both the release time period and the temporal profile are unknown, which presents a more complex challenge for source location estimation.

► Line 60-78 of section "1. Introduction" has been replaced with:

"*Assumptions on the release characteristics aim to reduce the dimension of the solution space to 4 or 5, i.e. the two source location coordinates, the total release, and the release time (or the release start and end time), by assuming that the substances are released instantaneously at a release time (or constantly during a release time period) (Kovalets et al., 2020, 2018; Efthimiou et al., 2018, 2017; Tomas et al., 2021; Andronopoulos and Kovalets, 2021; Ma et al., 2018). Under these assumptions, the correlation-based method has exhibited high accuracy for ideal cases under stationary meteorological conditions, such as synthetic simulation experiments (Ma et al., 2018) and wind tunnel experiments (Kovalets et al., 2018; Efthimiou et al., 2017). However, previous studies have also demonstrated that the application in real-world cases may be much more challenging, (Kovalets et al., 2020; Tomas et al., 2021; Andronopoulos and Kovalets, 2021; Becker et al., 2007), because the release usually exhibits temporal variations and may experience non-stationary meteorological fields. The interaction between the time-varying release characteristics and non-stationary meteorological fields is ignored in the instantaneous-release and constant-release assumption, leading to inaccurate reconstruction.*"

► Line 94-95 of section "1. Introduction" has been replaced with:

"The performance of the proposed method is compared with the correlation-based method ~~(constant-release assumption)~~ for source location estimation and the Bayesian method ~~(statistical assumption)~~ for spatiotemporal accuracy."

Comment#6:

Line 108: It is wrong to assume a square matrix. The dimensions of the observation and source vectors are independent and rarely the same.

Response to comment#6:

Thank you for pointing the error of the matrix. As you mentioned, the matrix **A(r)** is not a square matrix in general. We have modified the dimension of the matrix: $\mathbf{A}(\mathbf{r}) = [A_1(\mathbf{r}), A_2(\mathbf{r}), \cdots, A_N(\mathbf{r})]^T \in \mathbb{R}^{N \times S}$, where N is the number of sequential time steps and S is the length of release rate vector $\mathbf{q}$.

► Line 100-109 of section "2.1 Source reconstruction models" have been replaced with:

"For an atmospheric radionuclide release, Eq. (1) relates the observations at each observation site to the source parameters:

$$\boldsymbol{\mu} = \mathbf{F}(\mathbf{r}, \mathbf{q}) + \boldsymbol{\varepsilon}\,, \tag{1}$$

where $\boldsymbol{\mu} = [\mu_1, \mu_2, \cdots, \mu_N] \in \mathbb{R}^N$ is an observation vector composed of observations at N sequential time steps, the function **F** maps the source parameters to the observations, i.e. an atmospheric dispersion model, **r** refers to the source location, $\boldsymbol{q} \in \mathbb{R}^S$ is the temporally varying release rate, and $\boldsymbol{\varepsilon} \in \mathbb{R}^N$ is a vector containing both model and measurement errors.

In most source reconstruction models, **F** is simplified to the product of **q** and a source–receptor matrix **A** that depends on the source location:

$$\boldsymbol{\mu} = \mathbf{A}(\mathbf{r})\mathbf{q} + \boldsymbol{\varepsilon}\,, \tag{2}$$

where $\boldsymbol{A}(\boldsymbol{r}) = [A_1(\boldsymbol{r}), A_2(\boldsymbol{r}), \cdots, A_N(\boldsymbol{r})]^T \in \mathbb{R}^{N \times S}$ and each row describes the sensitivity of an observation to the release rate **q** given the source location **r**."

Comment#7:

Lines 122-124: The statement is not correct. The emissions combined with the meteorological conditions together determine the concentrations at any given measurement site, including the peak values and its timing.

Response to comment#7:

We agree that the emission and the meteorological jointly influence the peak values and its timing. Our work aims to smooth out the peak observations that is mainly shaped by the temporal release profile. We have restated our method based on this effect.

► Line 122-124 of section "2.2 Spatiotemporal decoupling" have been replaced with:

"With a fixed source location, *the release rate and meteorology jointly determine the temporal variation of the observations (Li et al., 2019). The influence of meteorology can be pre-calculated as source-receptor sensitivities and subsequently stored in matrix* $\boldsymbol{A}(\boldsymbol{r})$."

► Line 134-136 of section "2.3 Source localization without knowing the exact release rates" have been replaced with:

"After applying the filter in Eq. (4), *those peak observations that are mainly shaped by the temporal release profile, are smoothed out,* but the influences of the source position and meteorology remain relatively unchanged, as they determine the long-term temporal trends of observations and are less affected by the filter."

Comment#8:

Line 228: It is very confusing to use "sample" for the different candidate source locations.

Response to comment#8:

We apologize for any confusion caused by the term "sample". This term refers to an individual simulation using one of the candidate source locations. Therefore, each "sample" represents a simulated dispersion scenario with a different candidate source location. To clarify this point, we have replaced the word "sample" with "simulation" in the revised manuscript.

► Line 228-230 of section "2.6.2 Simulation settings of atmospheric dispersion model" have been replaced with:

"To establish the datasets for the XGBoost model, *2000 simulations and 1000 simulations with different source locations*

were performed by RIMPUFF for Oct. 3 and Oct. 4, respectively. The *candidate* source locations were *randomly* sampled from the shaded zones in Fig. 2a, which were determined according to the positions of the observation sites and the upwind direction. *Each simulation, along with its corresponding source location, forms one sample.*"

Comment#9

Lines 287-288: The hyper-parameters used in the 50 runs should be given in the supplementary document.

Response to comment#9:

We appreciate your suggestion regarding the inclusion of hyper-parameters. We have provided all hyper-parameters of the 50 runs in the revised version of the supplementary document.

Comment#10:

Figure S3: What is the sliding window applied here? It does seem to be a sided window rather than centered one. Please explain this in the paper.

Response to comment#10:

We apologize for the lack of clarity regarding the sliding window used in Figure S3. As outlined in Eq. (4), a one-sided window is employed. This one-sided temporal sliding-window average filter involves the current and previous observations in the window, acknowledging that future observations are not available for filtering in practice. Compared to the centered window, the one-sided window excels in real-time data processing and rapid response to changes in the observations, making it more suitable for real applications. Relevant descriptions of the sliding window have been modified in the revised manuscript for clarity.

► Line 128-132 of section "2.2 Spatiotemporal decoupling" have been replaced with:

"In this study, the following operator matrix is constructed to impose a *one-sided* temporal sliding-window average filter (Eamonn Keogh, Selina Chu, 2004):

$$\mathbf{P} = \frac{1}{T}\begin{bmatrix} 1 & & & & & & & & & \\ 1 & 1 & & & & & & & & \\ & \vdots & & & & & & & & \\ 1 & 1 & \cdots & 1 & & & & & & \\ 1 & 1 & \cdots & 1 & 1 & & & & & \\ & 1 & 1 & \cdots & 1 & 1 & & & & \\ & & 1 & 1 & \cdots & 1 & 1 & & & \\ & & & \ddots & \ddots & \ddots & \ddots & \ddots & & \\ & & & & 1 & 1 & \cdots & 1 & 1 & \\ & & & & & 1 & 1 & 1 & 1 & 1 \end{bmatrix}, \quad (4)$$

where T is the size of the sliding window. *This one-sided filter involves the current and previous observations in the window, acknowledging that future observations are not available for filtering in practice.* Although a sliding-window average filter is used in this study, Eq. (3) is compatible with more advanced processing methods."

Minor points

Comment#1:

Line 46, T3-10: Please explain what T3-10 distributions are.

Response to comment#1:

The notation T3-10 denotes a Student's *t*-distribution with degrees of freedom ranging from 3 to 10, as referenced in

(Wang et al., 2017). The *t*-distribution (also known as t_ν) is applicable for estimating the mean of a normally distributed population, when the sample size is small and the population standard deviation is unknown. In this distribution, the parameter ν represents the degrees of freedom and determines the distribution's shape. As ν increases, the *t*-distribution approaches the normal distribution. To eliminate the ambiguity, we have replaced "T3-10" with "*t-distribution (with degrees of freedom ranging from 3 to 10)*".

► Line 45-47 of section "1. Introduction" have been replaced with:

"Other candidates include *t-distribution (with degrees of freedom ranging from 3 to 10), Cauchy distribution, and log-Cauchy distribution*, which have been compared with normal and log-normal distributions in reconstructing the source parameters of the Prairie Grass field experiment (Wang et al., 2017)."

Comment#2:

Line 60: What does "deterministic assumption" mean? It is quite confusing.

Response to comment#2:

We apologize for any confusion caused by the term "deterministic assumption". Deterministic assumptions aim to define the physical feature of source parameters. A typical one is the constant-release assumption, which assumes that the substances are released at a constant rate during the release period (Kovalets et al., 2020, 2018; Efthimiou et al., 2018, 2017; Tomas et al., 2021; Andronopoulos and Kovalets, 2021; Ma et al., 2018). To avoid confusion, we have replaced the terms "Statistical assumption" and "Deterministic assumption" with "*Assumptions on model-observation discrepancies*" and "*Assumptions on the release characteristics*", respectively, in the introduction section in the revised manuscript.

► Line 38-78 of section "1. Introduction" have been replaced with:

"To reduce the problem of ill-posedness, most previous studies have attempted to constrain the reconstruction by imposing assumptions on *the model-observation discrepancies or release characteristics. Assumptions on model-observation discrepancies* are widely used in Bayesian methods to simultaneously reconstruct the posterior distributions of spatiotemporal source parameters (De Meutter et al., 2021; Meutter and Hoffman, 2020; Xue et al., 2017a). This assumes that the model–observation discrepancies follow a certain statistical distribution (i.e. the likelihood of Bayesian methods), with the normal (Eslinger and Schrom, 2016; Guo et al., 2009; Keats et al., 2007, 2010; Rajaona et al., 2015; Xue et al., 2017a, b; Yee, 2017; Yee et al., 2008; Zhao et al., 2021) and log-normal (Chow et al., 2008; Dumont Le Brazidec et al., 2020; KIM et al., 2011; Monache et al., 2008; Saunier et al., 2019; Senocak, 2010; Senocak et al., 2008) distributions being two popular choices. Other candidates include Cauchy, log-Cauchy, and *t* (with degrees of freedom ranging from 3 to 10) distributions, which have been compared with normal and log-normal distributions in reconstructing the source parameters of the Prairie Grass field experiment (Wang et al., 2017). The results demonstrate that the likelihoods are sensitive to both the dataset and the targeted source parameters. Some studies have constructed the likelihood based on multiple metrics that measure the model–observation discrepancies in an attempt to better constrain the solution (Lucas et al., 2017; Jensen et al., 2019). More sophisticated methods involve the use of different statistical distributions for the likelihoods of non-detections and detections (De Meutter et al., 2021; Meutter and Hoffman, 2020). Recent studies have suggested the use of log-based distributions and tailored parameterization of the covariance matrix as a means of better quantifying the uncertainties in the reconstruction (Dumont Le Brazidec et al., 2021). These Bayesian methods have been applied to real atmospheric radionuclide releases, such as the 2017 ^{106}Ru event, and have provided important insights into the source and release process (Dumont Le Brazidec et al., 2020; Saunier et al., 2019; Dumont Le Brazidec et al., 2021; De Meutter et al., 2021). However, these studies have also revealed that

the likelihood in Bayesian methods must be exquisitely designed and parameterized to achieve satisfactory spatiotemporal source reconstruction (Dumont Le Brazidec et al., 2021; Wang et al., 2017). With suboptimal design, the reconstruction may exhibit a bimodal posterior distribution (Meutter and Hoffman, 2020), which remains a challenge for robust applications in different scenarios.

Assumptions on the release characteristics aim to reduce the dimension of the solution space to 4 or 5, i.e. the two source location coordinates, the total release, and the release time (or the release start and end time), by assuming that the substances are released instantaneously at a release time (or constantly during a release time period) (Kovalets et al., 2020, 2018; Efthimiou et al., 2018, 2017; Tomas et al., 2021; Andronopoulos and Kovalets, 2021; Ma et al., 2018). Under these assumptions, the correlation-based method has exhibited high accuracy for ideal cases under stationary meteorological conditions, such as synthetic simulation experiments (Ma et al., 2018) and wind tunnel experiments (Kovalets et al., 2018; Efthimiou et al., 2017). However, previous studies have also demonstrated that the application in real-world cases may be much more challenging, (Kovalets et al., 2020; Tomas et al., 2021; Andronopoulos and Kovalets, 2021; Becker et al., 2007), because the release usually exhibits temporal variations and may experience non-stationary meteorological fields. The interaction between the time-varying release characteristics and non-stationary meteorological fields is ignored in the instantaneous-release and constant-release assumption, leading to inaccurate reconstruction."

Comment#3:

Figure 1: What do the different shapes and colors in the diagram mean?

Response to comment#3:

We apologize for not providing detailed explanations for the shapes and colors in Figure 1. We have added descriptions to the figure caption of the Fig. 1 and relabeled the root nodes using yellow squares in Fig. 1**,** providing a more accurate and detailed introduction to the decision tree model.

► Line 150-151 of section "2.3 Source localization without knowing the exact release rates" have been replaced with:

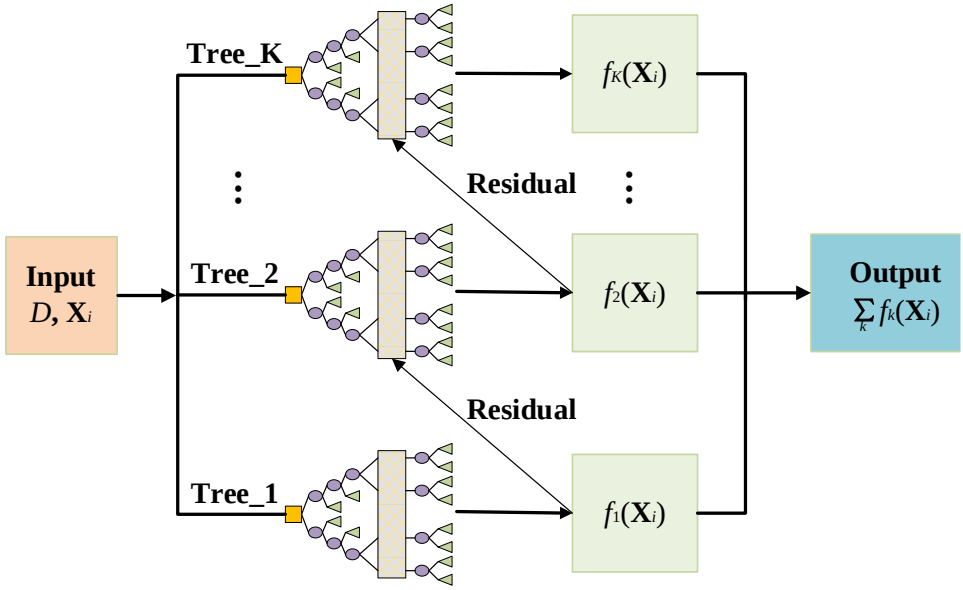

"**Figure 1.** Flowchart of XGBoost for predicting $\hat{\mathbf{r}}_i$ based on decision tree model. *The yellow squares are the root nodes within each tree, representing the input features in this paper. The purple ellipses denote the child nodes where the model evaluates input features and make decisions to split the data. The green rectangles depict the leaf nodes and refer to the prediction results. The vertical rectangles abstract the internal splitting processes of the trees, indicating decision-*

making not explicitly detailed in the diagram."

Comment#4:

Equation (7): Please explain all the parameters here.

Response to comment#4:

We appreciate your attention to Equation (7). To avoid confusion, we have replaced the symbol "T" with "M" in Eq. (7) and have provided additional descriptions for all the parameters.

► Line 147-157 of section "2.3 Source localization without knowing the exact release rates" have been replaced with: "where K is the number of trees, $\boldsymbol{\mathcal{F}} = \{f(x) = \boldsymbol{\omega}_{Q(x)}\}(Q: \mathbb{R}^p \to M, \boldsymbol{\omega} \in \mathbb{R}^M)$ is the space of decision trees, and Q represents the structure of each tree, mapping the feature vector to M leaf nodes. Each f_k corresponds to an independent tree structure Q with leaf node weight $\boldsymbol{\omega} = (\omega_1, \omega_2, \cdots, \omega_M)$. Equation (5) is then used to predict $\hat{\mathbf{r}}_i = (\hat{x}_i, \hat{y}_i)$ for the i-th sample.

XGBoost trains $G(\mathbf{X})$ in Eq. (5) by continuously fitting the residual error until the following objective function is minimized:

$$Obj^{(t)} = \sum_{i=1}^{n} \left(\mathbf{r}_i - \left(\hat{\mathbf{r}}_i^{(t-1)} + f_t(\mathbf{X}_i) \right) \right)^2 + \sum_{i=1}^{t} \Omega(f_i) \,, \tag{6}$$

where t represents the training of the t-th tree and $\Omega(f_i)$ is the regularization term, given by:

$$\Omega(f) = \Upsilon M + \frac{1}{2} \lambda \sum_{j=1}^{M} \omega_j^2 \,, \tag{7}$$

where M is the number of leaf nodes, ω_j is the leaf node weight for the j-th leaf node, Υ and λ are penalty coefficients.

The minimization of Eq. (6) provides the parametric model $G(\mathbf{X})$ that maps the feature ensemble $\mathbf{X}$ extracted from $\boldsymbol{\mu}_p$ to the source location $\mathbf{r}$."

Comment#5:

Line 160: Why is the amplitude quantity called "wave rate"?

Response to comment#5:

We apologize for the unclear definition. We aim to define the "wave_rate" as a statistical measure that quantifies the fluctuations of $\boldsymbol{\mu}_p$ over time. To reduce the impact of extreme values, the "wave rate" is calculated as the difference between the 90th and 10th quantiles of the normalized observation series. To avoid any ambiguity, we have removed the term "amplitude" from the revised manuscript and clarified the definition of "wave_rate" to ensure it accurately reflects the intended concept.

► Line 159-160 of section "2.3 Source localization without knowing the exact release rates" have been replaced with: "Among the time-domain features, the wave rate quantifies *the fluctuations of $\boldsymbol{\mu}_p$ over time without being overly influenced by extreme values*,"

Comment#6:

Lines 160-161: The median value is not a central moment.

Response to comment#6:

We appreciate your observation regarding the classification of median value. Upon reviewing relevant literature (Witte and Witte, 2017), the temporal mean and median values are indeed recognized measures of central tendency in statistical analysis. We have made revisions in the manuscript to clarify this point.

► Line 160-161 of section "2.3 Source localization without knowing the exact release rates" have been replaced with:

"while the temporal mean and median values *are measures of central tendency of* $\boldsymbol{\mu_p}$ *(Witte and Witte, 2017).*"

Comment#7:

Line 232: If it is 40th percentile, the number of samples for Oct.3 and Oct. 4 should be 1200 and 600.

Response to comment#7:

We appreciate your careful review and for identifying this discrepancy. Indeed, we intended to reference the 60th percentile, not the 40th. To clarify this point, we have revised our descriptions and instead specified that source locations corresponding to the highest 40% of correlation coefficients are selected for further analysis.

► Line 230-232 of section "2.6.2 Simulation settings of atmospheric dispersion model" have been replaced with:

"As described in Sect. 2.5.1, we calculated the correlation coefficient for each sample and *preserved 40% samples with the highest 40% of correlation coefficients* (i.e. 800 samples for Oct. 3 and 400 samples for Oct. 4)."

Comment#8:

Line 237: The authors probably mean 80th, 60th, 50th, 40th, 20th, and 0th.

Response to comment#8:

We appreciate your attention to this detail. You are correct. In line with the response to comment#7, we have revised the relevant descriptions to accurately reflect the search range.

► Line 236-238 of section "2.7 Sensitivity study" have been replaced with:

"The search range is controlled by the pre-screening threshold*, which is the top proportion of the correlation coefficients in the pre-screening step*. *Specifically, we use source locations corresponding to the highest 20%, 40%, 50%, 60%, 80%, and 100% of correlation coefficients to define search ranges, with a lower proportion indicating a narrower and more focused search area.*"

Comment#9:

Line 238: "A lower percentile" should be "a higher percentile".

Response to comment#9:

We appreciate your attention in identifying this discrepancy. We have corrected this error in the revised manuscript, which is consistent with the revisions discussed in comment#7 and comment#8.

Comment#10:

Figure 8: No shade appears for the Bayesian inversion results in the lower left panel.

Response to comment#10:

Thank you for pointing out the visualization issue regarding Fig. 8. To resolve this problem, we have enlarged the shading in this area for better visualization. Additionally, we have adjusted the shading range from [minimum, maximum] to [lower quartile, upper quartile] to better represent the results.

► Line 385-387 of section "3.3.3 Uncertainty range" have been replaced with:

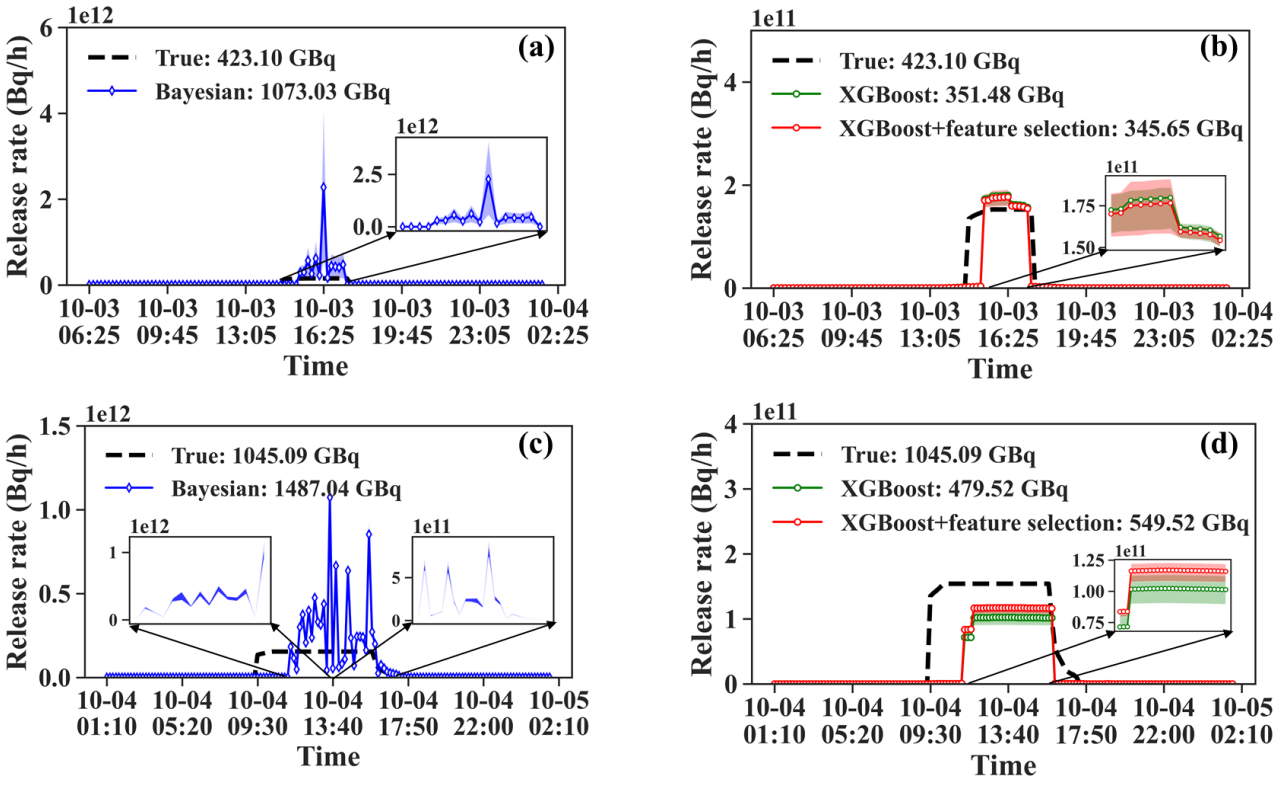

"**Figure 8.** Release rate estimates over 50 calculations *in SCK-CEN [41]Ar experiment*. *(a) Oct. 3-Bayesian method; (b) Oct. 3-The proposed methods; (c) Oct. 4-Bayesian method; (d) Oct. 4-The proposed methods. The shadow represents the uncertainty range between the lower quartile and the upper quartile. The shadow of each figure is amplified by an enlarged subgraph. The legends in each figure provide the mean estimates of total release.*"

Comment#11:

Line 416: What do the various pre-screening ranges refer to?

Response to comment#11:

We apologize for any confusion caused by the term "pre-screening ranges". These pre-screening ranges, as detailed in Sect. 2.5.1, refer to the specific subsets of source locations selected based on their correlation coefficients (i.e. search range). The pre-screening process is designed to reduce computational costs and eliminate low-quality samples by focusing on the most promising source locations for further analysis. To eliminate the ambiguity, we have replaced the "pre-screening ranges" with "*search ranges*".

► Line 403-404 of section "3.4.1 Sensitivity to the search range" have been replaced with:

"The error is smaller with a lower threshold, implying that a small *search range* helps reduce the mean and median errors."

► Line 415-417 of section "3.4.1 Sensitivity to the search range" have been replaced with:

"The mean/median error is less than 8% for Oct. 3 and less than 11% for Oct. 4, both of which are smaller than for the various *search ranges* in Fig. 9. This indicates that the proposed method is more robust to this parameter than to the *search range*."

Comment#12:

Figure S1: Should it be 20% instead of 10% for the five-fold cross-validation?

Response to comment#12:

We appreciate your attention to detail in Figure S1. You are correct about the discrepancy in the percentage for the five-fold cross-validation; it should be 20% instead of 10%. We have made this correction in the revised figure.

► Line 30-31 of Supplementary Material have been replaced with:

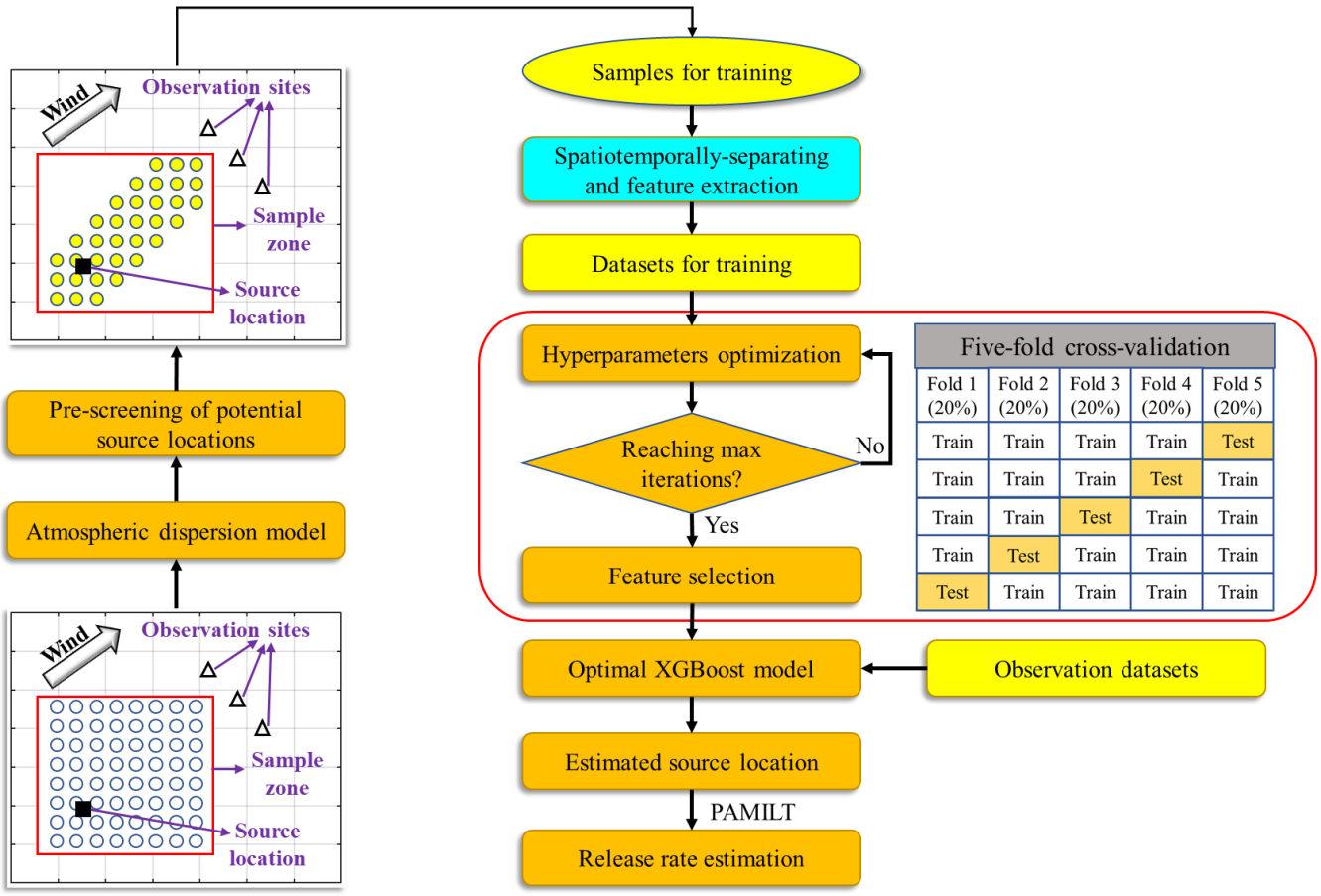

"**Figure S1.** Flowchart of the proposed *spatiotemporally-separated* source reconstruction method."

Comment#13:

Table S1: Brief descriptions of the hyperparameters should be provided.

Response to comment#13:

We appreciate your suggestion regarding Table S1. Brief descriptions of the hyperparameters have been included in the caption of Table S1 for clarity:

► Line 51 of Supplementary Material have been replaced with:

"Table S1. Hyperparameter optimization results. *max_depth-maximum depth of a decision tree; learning_rate-step size at each iteration while moving toward a minimum of the loss function; n_estimators-number of decision trees; min_child_weight-minimum sum of sample weight of a child node; subsample-subsample ratio of the training samples; colsample_bytree-subsample ratio of columns when constructing a tree; reg_lambda-L2 regularization term on weights; and gamma-minimum loss reduction required to split the tree.*"

Thanks again for such a thorough review!

References

Andronopoulos, S. and Kovalets, I. V.: Method of source identification following an accidental release at an unknown

location using a lagrangian atmospheric dispersion model, Atmosphere (Basel)., 12, 7–12, https://doi.org/10.3390/atmos12101305, 2021.
Becker, A., Wotawa, G., De Geer, L. E., Seibert, P., Draxler, R. R., Sloan, C., D'Amours, R., Hort, M., Glaab, H., Heinrich, P., Grillon, Y., Shershakov, V., Katayama, K., Zhang, Y., Stewart, P., Hirtl, M., Jean, M., and Chen, P.: Global backtracking of anthropogenic radionuclides by means of a receptor oriented ensemble dispersion modelling system in support of Nuclear-Test-Ban Treaty verification, Atmos. Environ., 41, 4520–4534, https://doi.org/10.1016/j.atmosenv.2006.12.048, 2007.
Bocquet, M.: Reconstruction of an atmospheric tracer source using the principle of maximum entropy. I: Theory, Q. J. R. Meteorol. Soc., 131, 2191–2208, https://doi.org/10.1256/qj.04.67, 2005a.
Bocquet, M.: Reconstruction of an atmospheric tracer source using the principle of maximum entropy. II: Applications, Q. J. R. Meteorol. Soc., 131, 2209–2223, https://doi.org/10.1256/qj.04.68, 2005b.
Chow, F. K., Kosović, B., and Chan, S.: Source inversion for contaminant plume dispersionin urban environments using building-resolving simulations, J. Appl. Meteorol. Climatol., 47, 1533–1572, https://doi.org/10.1175/2007JAMC1733.1, 2008.
Drews, M., Aage, H. K., Bargholz, K., Ejsing Jørgensen, H., Korsbech, U., Lauritzen, B., Mikkelsen, T., Rojas-Palma, C., and Ammel, R. Van: Measurements of plume geometry and argon-41 radiation field at the BR1 reactor in Mol, Belgium, 1–43 pp., 2002.
Dumont Le Brazidec, J., Bocquet, M., Saunier, O., and Roustan, Y.: MCMC methods applied to the reconstruction of the autumn 2017 Ruthenium-106 atmospheric contamination source, Atmos. Environ. X, 6, 100071, https://doi.org/10.1016/j.aeaoa.2020.100071, 2020.
Dumont Le Brazidec, J., Bocquet, M., Saunier, O., and Roustan, Y.: Quantification of uncertainties in the assessment of an atmospheric release source applied to the autumn 2017 106Ru event, Atmos. Chem. Phys., 21, 13247–13267, https://doi.org/10.5194/acp-21-13247-2021, 2021.
Eamonn Keogh, Selina Chu, D. H. and M. P.: SEGMENTING TIME SERIES: A SURVEY AND NOVEL APPROACH, in: Data mining in time series databases, 1–21, https://doi.org/10.1142/9789812565402_0001, 2004.
Efthimiou, G. C., Kovalets, I. V., Venetsanos, A., Andronopoulos, S., Argyropoulos, C. D., and Kakosimos, K.: An optimized inverse modelling method for determining the location and strength of a point source releasing airborne material in urban environment, Atmos. Environ., 170, 118–129, https://doi.org/10.1016/j.atmosenv.2017.09.034, 2017.
Efthimiou, G. C., Kovalets, I. V, Argyropoulos, C. D., Venetsanos, A., Andronopoulos, S., and Kakosimos, K. E.: Evaluation of an inverse modelling methodology for the prediction of a stationary point pollutant source in complex urban environments, Build. Environ., 143, 107–119, https://doi.org/10.1016/j.buildenv.2018.07.003, 2018.
Eslinger, P. W. and Schrom, B. T.: Multi-detection events, probability density functions, and reduced location area, J. Radioanal. Nucl. Chem., 307, 1599–1605, https://doi.org/10.1007/s10967-015-4339-3, 2016.
Guo, S., Yang, R., Zhang, H., Weng, W., and Fan, W.: Source identification for unsteady atmospheric dispersion of hazardous materials using Markov Chain Monte Carlo method, Int. J. Heat Mass Transf., 52, 3955–3962, https://doi.org/10.1016/j.ijheatmasstransfer.2009.03.028, 2009.
Jensen, D. D., Lucas, D. D., Lundquist, K. A., and Glascoe, L. G.: Sensitivity of a Bayesian source-term estimation model to spatiotemporal sensor resolution, Atmos. Environ. X, 3, https://doi.org/10.1016/j.aeaoa.2019.100045, 2019.
Keats, A., Yee, E., and Lien, F. S.: Bayesian inference for source determination with applications to a complex urban environment, Atmos. Environ., 41, 465–479, https://doi.org/10.1016/j.atmosenv.2006.08.044, 2007.
Keats, A., Yee, E., and Lien, F. S.: Information-driven receptor placement for contaminant source determination, Environ. Model. Softw., 25, 1000–1013, https://doi.org/10.1016/j.envsoft.2010.01.006, 2010.
KIM, J. Y., JANG, H.-K., and LEE, J. K.: Source Reconstruction of Unknown Model Parameters in Atmospheric Dispersion Using Dynamic Bayesian Inference, Prog. Nucl. Sci. Technol., 1, 460–463, https://doi.org/10.15669/pnst.1.460, 2011.
Kovalets, I. V., Efthimiou, G. C., Andronopoulos, S., Venetsanos, A. G., Argyropoulos, C. D., and Kakosimos, K. E.: Inverse identification of unknown finite-duration air pollutant release from a point source in urban environment, Atmos. Environ., 181, 82–96, https://doi.org/10.1016/j.atmosenv.2018.03.028, 2018.
Kovalets, I. V., Romanenko, O., and Synkevych, R.: Adaptation of the RODOS system for analysis of possible sources of

Ru-106 detected in 2017, J. Environ. Radioact., 220–221, https://doi.org/10.1016/j.jenvrad.2020.106302, 2020.
Krysta, M. and Bocquet, M.: Source reconstruction of an accidental radionuclide release at European scale, Q. J. R. Meteorol. Soc., 133, 529–544, https://doi.org/10.1002/qj.3, 2007.
Li, X., Sun, S., Hu, X., Huang, H., Li, H., Morino, Y., Wang, S., Yang, X., Shi, J., and Fang, S.: Source inversion of both long- and short-lived radionuclide releases from the Fukushima Daiichi nuclear accident using on-site gamma dose rates, J. Hazard. Mater., 379, 120770, https://doi.org/10.1016/j.jhazmat.2019.120770, 2019.
Lucas, D. D., Simpson, M., Cameron-Smith, P., and Baskett, R. L.: Bayesian inverse modeling of the atmospheric transport and emissions of a controlled tracer release from a nuclear power plant, Atmos. Chem. Phys., 17, 13521–13543, https://doi.org/10.5194/acp-17-13521-2017, 2017.
Ma, D., Tan, W., Wang, Q., Zhang, Z., Gao, J., Wang, X., and Xia, F.: Location of contaminant emission source in atmosphere based on optimal correlated matching of concentration distribution, Process Saf. Environ. Prot., 117, 498–510, https://doi.org/10.1016/j.psep.2018.05.028, 2018.
Meutter, P. De and Hoffman, I.: Bayesian source reconstruction of an anomalous Selenium-75 release at a nuclear research institute, J. Environ. Radioact., 218, 106225, https://doi.org/10.1016/j.jenvrad.2020.106225, 2020.
De Meutter, P., Hoffman, I., and Ungar, K.: On the model uncertainties in Bayesian source reconstruction using an ensemble of weather predictions, the emission inverse modelling system FREAR v1.0, and the Lagrangian transport and dispersion model Flexpart v9.0.2, Geosci. Model Dev., 14, 1237–1252, https://doi.org/10.5194/gmd-14-1237-2021, 2021.
Monache, L. D., Lundquist, J. K., Kosoví, B., Johannesson, G., Dyer, K. M., Aines, R. D., Chow, F. K., Belles, R. D., Hanley, W. G., Larsen, S. C., Loosmore, G. A., Nitao, J. J., Sugiyama, G. A., and Vogt, P. J.: Bayesian inference and Markov Chain Monte Carlo sampling to reconstruct a contaminant source on a continental scale, J. Appl. Meteorol. Climatol., 47, 2600–2613, https://doi.org/10.1175/2008JAMC1766.1, 2008.
Nodop, K., Connolly, R., and Girardi, F.: The field campaigns of the European tracer experiment (ETEX): Overview and results, Atmos. Environ., 32, 4095–4108, https://doi.org/10.1016/S1352-2310(98)00190-3, 1998.
Rajaona, H., Septier, F., Armand, P., Delignon, Y., Olry, C., Albergel, A., and Moussafir, J.: An adaptive Bayesian inference algorithm to estimate the parameters of a hazardous atmospheric release, Atmos. Environ., 122, 748–762, https://doi.org/10.1016/j.atmosenv.2015.10.026, 2015.
Saunier, O., Didier, D., Mathieu, A., Masson, O., and Dumont Le Brazidec, J.: Atmospheric modeling and source reconstruction of radioactive ruthenium from an undeclared major release in 2017, Proc. Natl. Acad. Sci. U. S. A., 116, 24991–25000, https://doi.org/10.1073/pnas.1907823116, 2019.
Senocak, I.: Application of a Bayesian inference method to reconstruct short-range atmospheric dispersion events, AIP Conf. Proc., 1305, 250–257, https://doi.org/10.1063/1.3573624, 2010.
Senocak, I., Hengartner, N. W., Short, M. B., and Daniel, W. B.: Stochastic event reconstruction of atmospheric contaminant dispersion using Bayesian inference, Atmos. Environ., 42, 7718–7727, https://doi.org/10.1016/j.atmosenv.2008.05.024, 2008.
Tomas, J. M., Peereboom, V., Kloosterman, A., and van Dijk, A.: Detection of radioactivity of unknown origin: Protective actions based on inverse modelling, J. Environ. Radioact., 235–236, 106643, https://doi.org/10.1016/j.jenvrad.2021.106643, 2021.
Ulimoen, M. and Klein, H.: Localisation of atmospheric release of radioisotopes using inverse methods and footprints of receptors as sources, J. Hazard. Mater., 451, https://doi.org/10.1016/j.jhazmat.2023.131156, 2023.
Wang, Y., Huang, H., Huang, L., and Ristic, B.: Evaluation of Bayesian source estimation methods with Prairie Grass observations and Gaussian plume model: A comparison of likelihood functions and distance measures, Atmos. Environ., 152, 519–530, https://doi.org/10.1016/j.atmosenv.2017.01.014, 2017.
Witte, R. S. and Witte, J. S.: Statistics, 496 pp., 2017.
Xue, F., Li, X., and Zhang, W.: Bayesian identification of a single tracer source in an urban-like environment using a deterministic approach, Atmos. Environ., 164, 128–138, https://doi.org/10.1016/j.atmosenv.2017.05.046, 2017a.
Xue, F., Li, X., Ooka, R., Kikumoto, H., and Zhang, W.: Turbulent Schmidt number for source term estimation using Bayesian inference, Build. Environ., 125, 414–422, https://doi.org/10.1016/j.buildenv.2017.09.012, 2017b.

Yee, E.: Automated computational inference engine for Bayesian source reconstruction: application to some detections/non-detections made in the CTBT international monitoring system, Appl. Math. Sci., 11, 1581–1618, https://doi.org/10.12988/ams.2017.74149, 2017.
Yee, E., Lien, F. S., Keats, A., and D'Amours, R.: Bayesian inversion of concentration data: Source reconstruction in the adjoint representation of atmospheric diffusion, J. Wind Eng. Ind. Aerodyn., 96, 1805–1816, https://doi.org/10.1016/j.jweia.2008.02.024, 2008.
Zhao, Y., Liu, Y., Wang, L., Cheng, J., Wang, S., and Li, Q.: Source Reconstruction of Atmospheric Releases by Bayesian Inference and the Backward Atmospheric Dispersion Model: An Application to ETEX-I Data, Sci. Technol. Nucl. Install., 2021, https://doi.org/10.1155/2021/5558825, 2021.